

## MASTER

### Heat and smoke removal in semi open car parks

an assessment of the fire-safety level when de designed using current guidelines on bases of worst case scenarios and wind effects

van der Heijden, M.G.M.

*Award date:*  
2011

[Link to publication](#)

#### **Disclaimer**

This document contains a student thesis (bachelor's or master's), as authored by a student at Eindhoven University of Technology. Student theses are made available in the TU/e repository upon obtaining the required degree. The grade received is not published on the document as presented in the repository. The required complexity or quality of research of student theses may vary by program, and the required minimum study period may vary in duration.

#### **General rights**

Copyright and moral rights for the publications made accessible in the public portal are retained by the authors and/or other copyright owners and it is a condition of accessing publications that users recognise and abide by the legal requirements associated with these rights.

- Users may download and print one copy of any publication from the public portal for the purpose of private study or research.
- You may not further distribute the material or use it for any profit-making activity or commercial gain

# Heat and smoke removal in semi open car parks

---

"An assessment of the fire-safety level when de designed using current guidelines  
on bases of worst case scenarios and wind effects"

By: M.G.M. van der Heijden<sup>1,2</sup> Advisors: prof. dr. ir. J.L.M. Hensen<sup>1</sup>, dr. ir. M.G.L.C. Loomans<sup>1</sup>, Ir. A.D. Lemaire<sup>2</sup>

<sup>1</sup>Eindhoven University of Technology, Eindhoven, Netherlands

<sup>2</sup>Efectis Nederland BV, Rijswijk, Netherlands



November 2010

## Abstract

If a design of a semi-open car park without a mechanical ventilation system doesn't meet the performance requirements stated in the Dutch building code directly, it is possible to show that the created design has an equal fire safety level as meant by this regulation. However it is questionable if the current guidelines meant to show this equivalence will ensure a satisfactory fire safety level in case of a car park fire, for every situation. In this paper a study is presented in which the fire safety level of semi-open car parks is analyzed by the use of different variants which are assessed on the fire safety level by validated Computational Fluid Dynamics (CFD) simulations. The results of this study show that it is possible to design a semi-open car park which complies with current existing guidelines, yet when assessed with the criteria for safe deployment of the fire department has an insufficient safety level. From the assessment of the influence of wind can be concluded that the presence of wind doesn't provide a higher safety level in all cases when compared to the same situation without wind. The latter being the generally assumed outdoor assessment condition.

# Table of Contents

<b>1</b>	<b>ACKNOWLEDGEMENTS</b>	<b>7</b>
<b>2</b>	<b>INTRODUCTION</b>	<b>8</b>
2.1	MOTIVATION FOR RESEARCH	8
2.2	BACKGROUND INFORMATION	9
2.2.1	FIRE SAFETY OF CAR PARKS	9
2.2.2	HAZARD SITUATIONS	11
2.3	DEFINITION OF A SEMI-OPEN CAR PARK	13
2.3.1	DESCRIPTION OF A SEMI-OPEN CAR PARK	13
2.3.2	DIFFERENT TYPES OF CAR-PARKS AND FOCUS	13
2.4	EXISTING DUTCH REGULATION AND GUIDELINES	14
2.4.1	GUIDELINE MANAGEABILITY OF FIRE	14
2.4.2	GUIDELINE NEN 2443	14
2.4.3	LNB GUIDELINE	15
2.4.4	ROTTERDAM PRACTICAL GUIDELINE	16
2.5	EXISTING GUIDELINES IN PRACTICE	16
2.6	COMPARISON WITH INTERNATIONAL GUIDELINES	17
<b>3</b>	<b>OBJECTIVE</b>	<b>18</b>
<b>4</b>	<b>METHOD</b>	<b>19</b>
4.1	PLENARY APPROACH	19
4.2	IDENTIFICATION OF GENERAL SEMI-OPEN CAR PARK DIMENSIONS	19
4.3	BASIC PRINCIPLES OF COMPUTATIONAL FLUID DYNAMICS	20
4.3.1	COMPUTATIONAL FLUID DYNAMICS IN GENERAL	20
4.3.2	TURBULENCE MODELS	21
4.3.3	WALL TREATMENT	22
4.3.4	WIND PRESSURE AND TURBULENCE INTENSITY	23
4.4	BASIC PRINCIPLES OF FIRE AND FIRE-MODELLING	27
4.4.1	POOL-FIRES	27
4.4.2	CAR-FIRES	27
4.4.3	SIGHT LENGTH THROUGH SMOKE	28
4.4.4	WEIGHTED SUM OF GRAY GASSES MODEL	29
4.4.5	THERMAL CAPACITY OF WALLS	30

<b>4.5</b>	<b>CASE STUDY FOR VALIDATION</b>	<b>31</b>
4.5.1	DESCRIPTION OF CASE STUDY	31
4.5.2	COMPARISON OF SIMULATION AND MEASUREMENTS	32
4.5.3	DETERMINATION OF SIMULATION CHARACTERISTICS	35
<b>4.6</b>	<b>TRANSITION FROM VALIDATION CASE TO CAR PARK SIMULATION</b>	<b>37</b>
4.6.1	DISCRIPTION OF TRANSITION CASE	37
4.6.2	COMPARISON OF SIMULATION AND TRANSITION CASE	37
<b>4.7</b>	<b>SET-UP OF SIMULATION OF SEMI-OPEN CAR PARKS</b>	<b>39</b>
4.7.1	IMPLEMENTATION OF OBTAINED RESULTS OUT OF TRANSITION CASE	39
4.7.2	HEAT AND SMOKE IMPLEMENTATION CHECK	40
<b>4.8</b>	<b>DIFFERENT SIMULATION VARIANTS</b>	<b>41</b>

<b>5</b>	<b>RESULTS</b>	<b>43</b>
5.1	TEMPERATURE SAFETY CRITERIA	43
5.2	SIGHT LENGTH SAFETY CRITERIA	46

<b>6</b>	<b>DISCUSSION</b>	<b>49</b>
6.1	ANALYSIS OF CAR PARK BEHAVIOR OVER TIME	49
6.1.1	EXPLANATION OF ANALYSIS APPROACH	49
6.1.2	IMPLEMENTATION OF ANALYSIS TO DIFFERENT VARIANTS	50
6.2	ANALYSIS ON BASES OF DIRECT COMPARISON ON SPECIFIC LOCATION	53
6.3	AREA OF CAR PARK WHICH IS APPROACHABLE FOR THE FIRE BRIGADE	54
6.4	SAFETY LEVEL ASSESSMENT FOR ALL VARIANTS	55

<b>7</b>	<b>CONCLUSIONS</b>	<b>56</b>
----------	--------------------	-----------

<b>8</b>	<b>RECOMMENDATIONS</b>	<b>57</b>
----------	------------------------	-----------

<b>9</b>	<b>REFERENCES</b>	<b>58</b>
----------	-------------------	-----------

<b>10</b>	<b>APPENDIXES</b>	<b>61</b>
-----------	-------------------	-----------

Appendix 1, determination of dimensions of structural bearings

Appendix 2, study on general car park dimensions

Appendix 3, determination of area for visibility towards fire

Appendix 4, Temperature at 1.8 [m] height over time

Appendix 5, Temperature at 2.3 [m] height over time

Appendix 6, Local sight length towards light reflecting object at 1.5 [m] height

Appendix 7, Local sight length towards light reflecting object at 1.0 [m] height

Appendix 8, Local sight length towards light source at 1.5 [m] height

Appendix 9, Local sight length towards light source at 1.0 [m] height

## Symbols

$K$	=	Von Karman constant (0.42) [-]
$\dot{q}_{irr}$	=	Irradiation heat flux [ $\text{Wm}^{-2}$ ]
$\dot{Q}$	=	Heat release [kW]
$T_{\infty}$	=	Starting temperature [ $^{\circ}\text{C}$ ]
$U_{ABL}^*$	=	Friction velocity [ $\text{m}^1\text{s}^{-1}$ ]
$\mu$	=	Dynamic viscosity [ $\text{kg}^1\text{m}^{-1}\text{s}^{-1}$ ]
$A$	=	Total floor area of the building [ $\text{m}^2$ ]
$C_a$	=	The CO-content of the in the supplied air [%]
$C_p$	=	Wind induced pressure coefficient [-]
$d$	=	Diameter of pan fire [m]
$E$	=	Margin of error (15%) [%]
$F$	=	Fire frequency [ $\text{year}^{-1}$ ]
$f$	=	Vehicle fire frequency per visit [ $\text{visit}^{-1}$ ] ( $1.71 \cdot 10^{-7}$ according to §2.3.1)
$H$	=	Ceiling Height [m]
$I_u$	=	Turbulent intensity [%]
$K$	=	Constant for a particular type of the building [-]
$k(y)$	=	Turbulent kinetic energy [ $\text{m}^2\text{s}^{-2}$ ]
$n$	=	The number of cars present in the car park with running engine [-]
$N$	=	Minimal spot check size [-]
$N'$	=	corrected minimal spot check size for relative small populations [-]
$n_{pop}$	=	magnitude of population (1012) [-]
$OSD$	=	Optical smoke density [ $\text{m}^{-1}$ ]
$p$	=	percentage of specified category (worst case 50%) [-]
$P$	=	Heat release of fire [W]
$P_{co}$	=	The average CO production of a running engine ( $P_{co}=0.35$ ) [ $\text{m}^3\text{h}^{-1}$ ]
$P_{eff}$	=	Efficiency of parking [ $\text{m}^2\text{space}^{-1}$ ]
$PI_x$	=	Percentage of people that will obtain injury [%]
$PR_1^{st \text{ degree burn}}$	=	Probit of people that will obtain a 1 <sup>st</sup> degree burn [-]
$PR_2^{nd \text{ degree burn}}$	=	Probit of people that will obtain a 2 <sup>nd</sup> degree burn [-]
$PR_{lethal}$	=	Probit of people for which the irradiation dose is lethal [-]
$P_s(y)$	=	Dynamic pressure at height $y$ [pa]
$q$	=	The ventilation amount [ $\text{m}^3\text{h}^{-1}$ ].
$R$	=	Annual usage ratio of the parking building [ $\text{visit}^1\text{year}^{-1}\text{space}^{-1}$ ]
$r$	=	Distance from fire [m]
$RMS$	=	Root mean square of error is percents [%]
$RR$	=	Regression rate [ $\text{mm}^1\text{min}^{-1}$ ]
$S^*$	=	Irradiation dose [ $\text{J}^{4/3}\text{s}^{-1/3}\text{m}^{-2}$ ]
$SL_l$	=	Sight length towards a light source [m]
$SL_{lr}$	=	Sight length towards light reflecting object [m]
$SL_{prac}$	=	Sight length defined by the Dutch practical guideline [m]
$t$	=	Time [s]
$T$	=	Temperature [ $^{\circ}\text{C}$ ]
$TGG_{30min}$	=	The CO content with maximum ventilation amount ( $\text{CO} \leq 120$ ppm) [%].
$U$	=	Velocity [ $\text{m}^1\text{s}^{-1}$ ]
$U(y)$	=	Velocity at height $y$ [ $\text{m}^1\text{s}^{-1}$ ]
$w$	=	Percentage of non-specified category (worst case 50%) [-]
$X_{cfd}$	=	Temperature found with CFD simulation [ $^{\circ}\text{C}$ ]
$X_{measurement}$	=	Temperature found with measurements [ $^{\circ}\text{C}$ ]
$y$	=	Distance of first node to wall [m]
$y$	=	Vertical coordinate [m]
$Y^*$	=	Y-plus value or dimensionless wall distance [-]
$y_o$	=	Aerodynamic roughness length [m]
$z$	=	z-value at the desired reliability (99%, $z=2.57$ ) [-]
$\alpha$	=	Constant for a specific building [-]
$\rho$	=	Density of fluid [ $\text{kg}^1\text{m}^{-3}$ ]
$\rho$	=	Density of liquid [ $\text{kg}^1\text{m}^{-3}$ ]
$\rho_o$	=	Ambient outdoor air density [ $\text{kg}^1\text{m}^{-3}$ ]
$\tau_w$	=	Sheer stress in first node from wall [ $\text{N}^1\text{m}^{-2}$ ]
$\varepsilon(y)$	=	Turbulent dissipation velocity at height $y$ [ $\text{m}^2\text{s}^{-3}$ ]
$\sigma$	=	High heating value [ $\text{J}^1\text{kg}^{-1}$ ]

# 1 Acknowledgements

In the past year I worked on this graduation project, the achievement however wasn't possible without the support, suggestions, critical comments and shared experience of my supervisors. Therefore I'm pleased to thank prof.dr.ir. Jan Hensen, dr.ir. Marcel Loomans from the Eindhoven University of Technology and ir. Tony Lemaire from Efectis Nederland B.V. for their shared knowledge during the course of this project.

During my graduation project I spend most of the time in the Efectis office where next to my graduation project I worked for 8 hours a week. I shared working hours, lunches and dinners with most of the colleagues who I would like to thank for their suggestions and for making the experience more enjoyable. A special appreciation goes out to ir. Ingrid Naus, Johnny Ostfeldt MSc. and Wim Fokker for their different insights, sharing of life experiences and overall support. Thanks to them I managed to hold on to the project in unlucky times when the desired results weren't obtained or the logic seemed miles away.

In the finalization of this project I was able to spend a considerable amount of time at the Eindhoven University of Technology where I could work together with my friends from study association Mollier. I would like to thank all of them for their support and shared interest in the project.

Finally, I would like to thank my two grandmothers, parents and brother who even in the toughest times provided me with more love, believe and patience than I could ever have wished for.



Mike van der Heijden  
October 2010

## 2 Introduction

In this thesis first the motivation for the research is provided after which background information on car fire statistics and the Dutch regulation are presented. In the following paragraph a description of the objective is provided, in which the research question and sub questions are stated. The methodology will be discussed in the following paragraph where the case study for validation of the CFD-model and different variants for simulation are introduced. In the following paragraph the results of the different variants are presented which are discussed and analyzed in the next paragraph. Finally the research question will be answered in the last paragraph.

### 2.1 Motivation for research

The number of motorized vehicles in the Netherlands grows constantly. Based on figures obtained from the Central Bureau of Statistics (CBS) in the Netherlands it appears that in the last 6 years the number of motorized vehicles grew from 9.3 million to over 10.3 million [1]. Meaning an increase of nearly 11% in the past 6 years. Moreover it appears that 75% of these motorized vehicles are cars [2]. These cars have to be parked eventually, resulting in a constant growth of car park area in the Netherlands. This car park area can be created in an open field, however due to the urbanisation and ground cost it is more efficient to build car parks in most of the cases. These car parks can either be mechanically- or naturally ventilated, in which naturally ventilated car parks are more cost efficient in most cases. If the latter is the case, then it has to be considered that the walls of this car park need to have a certain opening area which is directly linked to the outside air. This is necessary in order to obtain the desirable amount of fresh air, and to extract the carbon monoxide which is created by the cars. Moreover the amount of open façade should be large enough to ensure that heat and smoke is removed effectively in case of a car fire in order to obtain a safety level which is in line with Dutch regulations. If this regulation is taken into account it can be noted that most car parks do not meet the requirements directly, which is caused by the large surface areas inside a car park which results in fire compartments which are too large according to the Dutch building decree. The way to deal with is, is to show that an equal safety level is still obtained as meant by the Dutch building decree, for which different guidelines exist. In this report the applicability of these different guidelines is discussed, moreover since the guideline which is commonly used for semi-open naturally ventilated car parks (NEN2443) is based on the amount of ventilation instead of the heat and smoke removal, it is assessed if the safety level obtained is of an appropriate level.



## 2.2 Background information

### 2.2.1 Fire safety of car parks

Several studies are focused on specific trends and frequencies in car park fires. These studies will be discussed in this paragraph.

#### Trends in car park fires

Based on a research on U.S. vehicle fire trends and patterns in 2002 [3] it appeared that there were about 329,500 vehicle fires that year, which caused 565 civilian deaths, 1,825 civilian injuries and \$1,392,000,000 in direct property damage. It could be concluded that 20% of all the occurred fires in the US that year were vehicle fires which caused 17% of all civilian fire deaths, 10% of all civilian fire injuries and 13% of the nation's property loss to fire. It appeared that more people died from vehicle fires than was the case with apartment fires, and as much as seven times the number of deaths caused by non-residential structure fires. It has to be noticed however that this involved all the vehicle fires, in- and outside car parks.

In the last decades also a large amount of vehicle fires have been reported inside car parks [4][5][6][7][8], and several investigations have been performed to the cause and effects of a car park fires.

In the Netherlands there were 32 fires in car parks over the years 2006, 2007 and 2008 [4] which makes an average of 10.7 fires per year. For 62% of the cases it is unknown what triggered the fire, for the other 25% and 13% it was respectively vandalism and short-circuit of an electric system. The place where the fire started was localized in one or more vehicles in 68% of the cases, in 16% of the cases the fire didn't start in a car and in 16% the location was not known. The average amount of cars involved in a car park fire was 3.1 cars. In 12% of the car park fires there were injuries but fortunately not fatal. The average involved vehicles and objects can be seen in Fig. 1

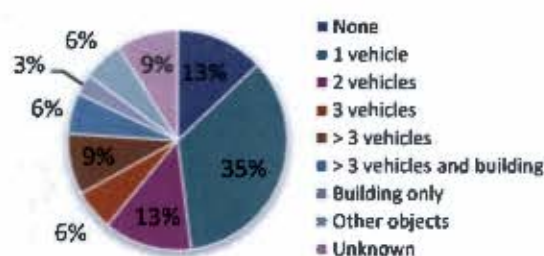


Fig. 1. Damage caused by car park fire [4].

Based upon a total of 405 car park fires which were reported by the Fire brigade of Paris [5] it appeared that it is most likely that there is only one car on fire. Moreover out of this report could also be concluded that it is unlikely that there are more than three cars on fire. In the report a distinction is made between underground car parks and open car parks. The amount of cars on fires in an underground car parks can add up to a total of 7, where in an open car park there weren't any cases in which more than 3 cars were on fire. However it could also be noticed that in an open car park there was a higher possibility that there was more than one car on fire as visible in Fig. 2 (were the percentage of occurrence is set as a function of the number of burning cars). It

was noticed that in 30% of the cases the fire wasn't a result of the cars but rather from garbage, paper or other combustibles. It could also be noticed that there were 12 non fatal injuries reported. Based upon a similar research in Berlin, were 31 car park fires were examined it could be concluded that there was a low probability that there were more than three cars on fire [5]. Out of an assessment of vehicle fires in New Zealand [6] could be concluded that there are on average about 3.371 vehicles on fire in New Zealand each year, this is based upon fire reports over the eight year period from 1995 to 2003. From the fires in this period there were about 101 fires in parking buildings which makes an average of 12.8 fires in car parks per year in New Zealand. The report also makes an estimation of the possibility of a carpark fire, which is  $1.7 \cdot 10^{-7}$  visit<sup>-1</sup> or one fire per  $5.9 \cdot 10^6$  visits. It was determined that in 92% of the cases only one car was involved in the fire, in 2% two cars and four cars in 1% of the cases, in the other 5% there wasn't a car involved. The causes of the fires were also examined. This provided the results as shown in Fig. 3. The trend of cases in which the fire was deliberately lit, is comparable to the Dutch trend. Based upon reported car park fires in the UK [7] it could be seen that over a 12 year period (1994-2005) there were 2 fatalities and 87 non fatal injuries as a result of car park fire (7 injured people per year). Most of the recorded fires didn't spread (from one car to another). It was also concluded that car-park fires represented a small percentage of all the fires in the UK. In the year 2006 the number represented less than 0.1% of the total fires in the UK.

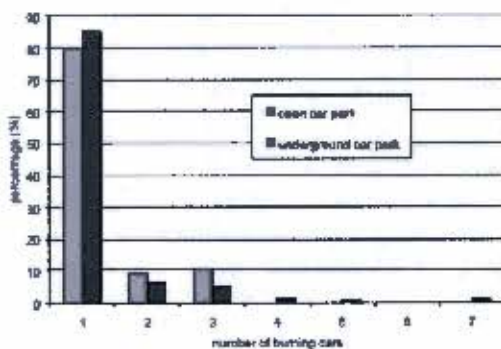


Fig. 2. Percentage of burning cars in an open and closed car park [5]

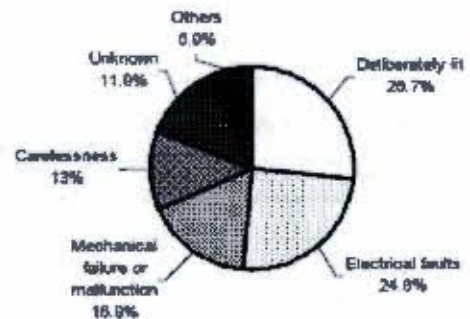


Fig. 3. Supposed causes of vehicles fires in parking buildings [6].

#### Fire frequency in relation to surface area

It appeared that there has been a variety of studies on the fire frequency in a building. It could be noticed that there is a correlation between the fire frequency, the surface area of the building and the particular type of building. This correlation can be expressed by the following equation [8][9].

$$F = K \cdot A^\alpha \quad (1)$$

In which:

- $F$  = Fire frequency [year<sup>-1</sup>]
- $K$  = Constant for a particular type of the building [-]
- $A$  = Total floor area of the building [m<sup>2</sup>]
- $\alpha$  = Constant for a particular type of the building [-]

The constants for the manufacturing industry, storage and offices are known [10] and visible in Table 1. Out of this can be concluded that a fire is most likely to occur in industry if the surface area is smaller than  $\pm 8.800\text{m}^2$  for larger floor areas this is the case for offices.

Table 1. Constants of K and  $\alpha$  for various occupancies [10].

Constant	Manufacturing industry	Storage	Offices
K	$1.70 \cdot 10^{-3}$	$6.70 \cdot 10^{-4}$	$5.9 \cdot 10^{-5}$
$\alpha$	0.53	0.5	0.9

The fire frequency in parking buildings is based on the surface area and usage ratio of a parking building. The equation for the fire frequency in car parks is defined for New Zealand as depicted below [6].

$$\left. \begin{aligned} F &= K \cdot A^\alpha \\ K &= \frac{f \cdot R}{P_{eff}} \end{aligned} \right\} \Rightarrow F_{\alpha=1} = f \cdot R \cdot \frac{A}{P_{eff}} \quad (2)$$

In which:

- $f$  = Vehicle fire frequency per visit [ $\text{visit}^{-1}$ ] ( $1.71 \cdot 10^{-7}$  as discussed in §2.3.1)
- $R$  = Annual usage ratio of the parking building [ $\text{visit}^1 \text{year}^{-1} \text{space}^{-1}$ ]
- $A$  = Total floor area of the building [ $\text{m}^2$ ]
- $P_{eff}$  = Efficiency of parking [ $\text{m}^2 \text{space}^{-1}$ ] (29 according to [11])

Bases on the New Zealand research  $f$  and  $R$  could be determined.  $R$  is defined as annual vehicle visits to a particular parking building divided by total number of parking spaces in this parking building. Based on the number of parking visits to a car park in Christchurch city (second largest city in New Zealand with an urban population density of  $854 \text{ [people}^1 \text{km}^{-2}]$  [12]) with 3,164 parking spaces and  $\pm 1.1 \cdot 10^6 \text{ visits}^1 \text{year}^{-1}$  (based on statistics of 2003) the annual usage ratio ( $R$ ) is determined to be 350 [ $\text{visit}^1 \text{year}^{-1} \text{space}^{-1}$ ] [6]. The result of equations (2) as described above is shown in Fig. 4 in which on the horizontal axes the surface area of the car park is stated and on the vertical axes the annual fire frequency. Next to the discussed cases also a case is plotted in which the usage ratio is four times higher as derived from the car park in Christchurch city. This line is based on the difference in population density between Christchurch city and Amsterdam, where the urban population in New Zealand is  $854 \text{ [people}^1 \text{km}^{-2}]$  it is about  $3,500 \text{ [people}^1 \text{km}^{-2}]$  in Amsterdam [13]. The rough indication in which it is assumed that the amount of parking spaces is proportional to the people density and eventually proportional to usage ratio and surface area, is given by this line. And is only determined to make the sensitivity to the usage ratio and surface area visible.

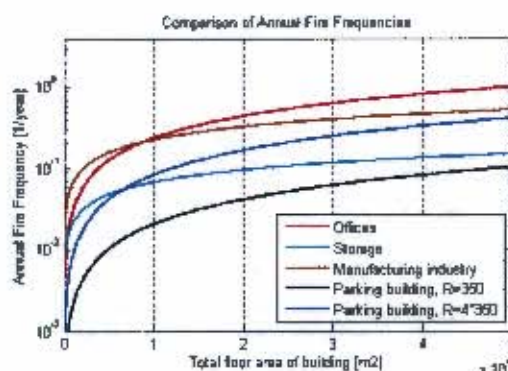


Fig. 4. Comparison of annual fire frequencies.

## 2.2.2

### Hazard situations

The most safe situation concerning fire safety would be described as a case in which a fire doesn't occur at all, however as described in previous paragraph this isn't a likely case to happen. Moreover it is even questionable if it is possible to create such a situation from an economical, esthetical and functional point of view [14]. Since it appears to be unavoidable that a fire will

develop at one time in a particular building, it is necessary to assess which factors cause a hazard situation in case of a fire. In literature three criteria for non-enclosed places with a short stay function are used, these are [15]:

- 1) A maximum irradiative heat flux from the smoke layer of 1 [kW<sup>1</sup>m<sup>-2</sup>].
- 2) A temperature below 45 [°C].
- 3) A minimal sight length of 100 [m].

However there are also criteria which indicate that a more perilous situation can still be qualified as safe for evacuation, the maximum conditions can for example also be limited to [16]:

- 1) A maximum irradiative heat flux at head height from the smoke layer of 2.8 [kW<sup>1</sup>m<sup>-2</sup>].
- 2) A maximum smoke layer temperature of 200 [°C].
- 3) A minimal sight length of 30 [m].

The difference between these two can be explained by the different meaning of staying somewhere for a short time and being somewhere in case of an evacuation. It can be discussed that in case of an evacuation minor injuries are still accepted in contrast to staying somewhere for a short time. The impact of a higher temperature and irradiation heat flux is linked to the exposure time. This exposure time in relation to the irradiation is called the irradiation dose and can be calculated by multiplying the time with the irradiation to the power 4/3 (equation 3). Next to this equation also the relations between the irradiation dose and consequence on a naked human skin is shown. This is displayed in Fig. 5 [17].

$$S^* = t \cdot \dot{q}_{irr}^{\frac{4}{3}} \quad (3)$$

$$PR_{1^{st} \text{ degree burn}} = -39.83 + 3.0186 \cdot \ln(S^*) \quad (4)$$

$$PR_{2^{nd} \text{ degree burn}} = -43.14 + 3.0186 \cdot \ln(S^*) \quad (5)$$

$$PR_{lethal} = -36.38 + 2.5600 \cdot \ln(S^*) \quad (6)$$

$$PI = 50 \cdot \left[ 1 + \left( \frac{PR-5}{|PR-5|} \right) \cdot \operatorname{erf} \left( \frac{|PR-5|}{\sqrt{2}} \right) \right] \quad (6)$$

In which:

- $S^*$  = Irradiation dose [ $J^{4/3} s^{-1/3} m^{-2}$ ]
- $t$  = Time [s]
- $\dot{q}_{irr}$  = Irradiation heat flux [ $Wm^{-2}$ ]
- $PR_{1^{st} \text{ degree burn}}$  = Probit of people that will obtain a 1<sup>st</sup> degree burn [-]
- $PR_{2^{nd} \text{ degree burn}}$  = Probit of people that will obtain a 2<sup>nd</sup> degree burn [-]
- $PR_{lethal}$  = Probit of people for which the irradiation dose is lethal [-]
- $PI_x$  = Percentage of people that will obtain injury [%]

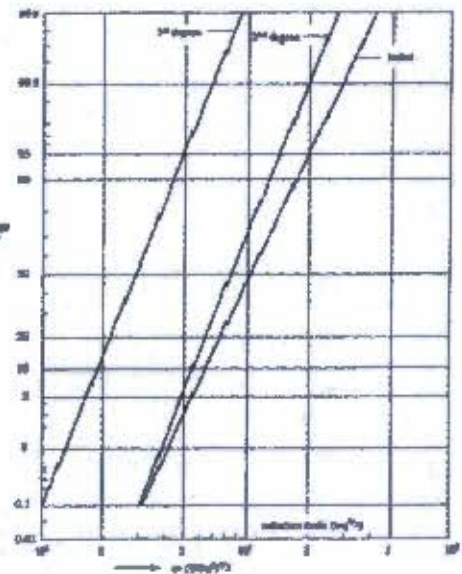


Fig. 5. Injury versus irradiation dose

For example when a radiation dose of  $1.05 \times 10^7 [J^{4/3} s^{-1/3} m^{-2}]$  is obtained, it appears that for 50% of people this will be lethal. This radiation dose is reached when a person is exposed to 20 [kW<sup>1</sup>m<sup>-2</sup>] for 20 seconds or to 5.8 [kW<sup>1</sup>m<sup>-2</sup>] for 100 seconds.

For the safe deployment of the fire brigade more severe limits of safety could be considered due to the proper gear and clothing of the fire brigade. The following safety criteria are considered for firemen [18][19][20].

- 1) A maximum temperature at 1.8 [m] height of 100 [°C].
- 2) A maximum temperature at 2.3 [m] height of 270 [°C] (smoke layer temperature).
- 3) A minimal sight length of 30 [m].
- 4) A maximum irradiative heat flux from the smoke layer of 5 [kW<sup>1</sup>m<sup>-2</sup>], which is the maximum irradiation if the temperature of the smoke layer is 270 [°C].

Considering the sight length the height at which this is observed has a significant influence. In the Rotterdam practical guideline the 30 meter sight at 2.5 meter is required. However in practise a height of 1.5 meter is accepted by most civil communities. Moreover in the concept NEN6098 a height of 1 meter is required. Due to these differences both a height of 1.5 [m] as 1 [m] is taken into account. Final conclusions however are based on 1.5 [m] height.

## 2.3 Definition of a semi-open car park

In this chapter a description of a semi-open car park will be provided, moreover different types will be discussed. Eventually the type on which will be focus in this research is provided.

### 2.3.1 Description of a semi-open car park

A uniformly used definition of a semi-open car park doesn't exist. In this research a car-park will be considered as semi-open when it has walls which have openings directly linked to the outside air. Moreover this amount of open area is large enough that there isn't a mechanically ventilation systems required for the heat and smoke removal. This amount is based on current Dutch guidelines.

### 2.3.2 Different types of car-parks and focus

When car parks are observed it is possible to make a distinction between different types [21]. These are split-level decks, sloping parking decks and flat decks which are sketched in Fig. 6 to Fig. 8. These three types have a rectangular shape but could potentially have a significantly different influence on the heat and smoke removal. In split-level decks heat and smoke does potentially travel quite easily throughout the entire car park. In sloping parking decks this would potentially also be the case, however the smoke is most likely to travel in one direction due to buoyancy effects. The type of car-park focused on in this report is the flat deck. Meaning that the parking deck is completely horizontal and heat/smoke can't travel to another floor other than by a ramp.



Fig. 6. Split-level decks



Fig. 7. Sloping decks



Fig. 8. Flat decks

## 2.4 Existing Dutch regulation and guidelines

The Dutch regulation concerning fire-safety is defined in the Dutch building decree [22]. This regulation makes a distinction between two demands, namely the performance requirements and the prescriptive requirements. Every section of the ordinance starts with a performance demand after which a description is given on how this performance demand can be met. The later is called the prescriptive requirement.

Alternative solutions are allowed based on the equivalence principle, meaning that an equal or better performance than required is shown through objective assessments. The way in which this equivalence can be adduced however, isn't prescribed in the Dutch building decree. Moreover, the municipality isn't authorised to prescribe how it shall be done (this is written in staatsblad 410 [23]).

There exist some guidelines which can be used to show equivalence when dealing with car parks. These guidelines will be discussed in the following subparagraphs.

### 2.4.1 Guideline manageability of fire

The method described in this guideline is meant to show equivalence by the manageability of a fire [24]. When the method is implemented it ensures that during the lifespan of a fire, the fire is maintained within the fire compartment. Therefore the guideline handles two requirements, namely a requirement on the amount of combustible material present in the fire compartment, and a requirement on the envelope of the fire compartment

### 2.4.2 Guideline NEN 2443

This guideline formulates performance- and prescriptive requirements for the parking of passenger cars on terrain and in garages [25]. Only a relative small part of the guideline is oriented on fire safety. The guideline regards elements as the electrical installation (for example the emergency lights and emergency power supply), ventilation and security system (like evacuation alarm, dry extinguish tubing and fire extinguishers)

This guideline is often used to determine if a car parking can be regarded as a naturally ventilated (open) car parks. According to this guideline this can be defined in two ways:

- 1) When all the following conditions are met:
  - a) At least two opposite walls must be outside walls and provided with openings that can't be closed from the outside air.
  - b) The outside opposite walls can't be more than 54 meter away from each other.
  - c) The lowest floor isn't more than 1.4 meter below ground level.
  - d) The inside walls may not form a restraint for the ventilation (this can be calculated by the use of NEN1087 [26]).
  - e) One of the two following requirements has to be met:
    - i) All opposite openings that can't be closed from the outside air need to have a total surface area of at least  $\frac{1}{3}$  of the total surface of the walls in the fire compartment.
    - ii) All opposite openings that can't be closed from the outside air each need to have a total surface area of at least 2.5% of the total surface area of the garage floor in the fire compartment.

- 2) When the foregoing conditions aren't met but it can be demonstrated that the ventilation capacity is satisfactory (for instance by the use of an airflow network model or NEN1087). The demanded ventilation capacity can be determined in two ways, namely:
- From the building code division 3.10 article 3.48 [22] which states that for an edifice with a function to park motor vehicles should have a ventilation capacity of 3 liter per second per square meter surface area.
  - In the NEN2443 an equation is stated which can also provide the air flow amount, this equation is based on a maximum CO-concentration which is allowable in a car park. This is equation is:

$$q = \frac{n \cdot P_{CO} \cdot 10^3}{TGG_{30min} - C_a} \quad (7)$$

In which:

- |               |   |   |
|---------------|---|---|
| $q$           | = | The ventilation rate ( $m^3h^{-1}$ ).   |
| $n$           | = | The number of cars per hour which are present in the car park with a running engine [-] This can be determined from publication "Handboek installatietechniek" [27] |
| $P_{CO}$      | = | The average CO production of a running engine ( $P_{CO}=0.35 [m^3h^{-1}]$ ).  |
| $TGG_{30min}$ | = | The CO content (time scaled average) with maximum ventilation amount ( $CO \leq 120$ ppm) [‰].  |
| $C_a$         | = | The CO content of the in the supplied air (which has to be determined out of measurements on location) [‰]  |

### 2.4.3 LNB Guideline

The LNB guideline [28] gives supplementary fire safety requirements on the building code for car parks larger than  $1000 m^2$ . It provides a combined approach for evacuation, compartmenting and fire fighting for new designed car parks, which is in mainly oriented on an effective and safe deployment of a fire brigade. The guideline is aggravated on mechanically ventilated garages.

The following supplementary fire safety requirements are given in the LNB guideline.

- Walking distances from any point in the car park to an exit is maximum 30 meter.
- When the lowest floor is more than 8 meters below ground level, a higher fire-resistant to collapse of the structural work is required.
- Structural parts have to satisfy fire propagation class 1.
- Evacuation signs have to be located both high and low.
- Fire hoses have to be present and capable to cover the complete car park.
- In a stairwell dry fire hoses have to be present.
- In case of a fire there has to be ventilation, this can be natural or mechanical as long as the capacity is sufficient.

In the table depicted below the relation between the surface area of a car park and the required amount of fresh air can be seen. In the case that a CFD-simulation has to be preformed, the intention is to show that 45 minutes after the start of a fire the sight length is at least 30 meters.

Table 2: Required ventilation amount according to the LNB guideline

Surface area	Ventilation amount
$\leq 1000 \text{ m}^2$	According to Dutch building code afd. 3.10. The required ventilation capacity is depicted for the different functions a building can have.
$> 1000 \leq 5000 \text{ m}^2$	10 times per hour.
$> 5000 \text{ m}^2$	A CFD-simulation has to be performed.

#### 2.4.4 Rotterdam practical guideline

This guideline is comparable to the LNB guideline, however some differences exist in the requirements [29]. These differences are:

- 1) The walking distances have to meet the performance requirements of the building code 2003 instead of the 30 meters stated in the LNB guideline.
- 2) A dividing wall between an enclosed room and the stairwell which is more than 8 meters below surface has to have a fire resistance of at least 60 minutes.
- 3) It has to be avoided that evacuation routes coincide.
- 4) Dry fire hoses have to be present if the floor is higher than 20 meters or lower than 8 meters from the surface. Moreover the couplings for the hoses need to be placed at the entrance hall of the stairwell.
- 5) Next to fire hoses also other forms of (portable) extinguish equipment is allowed (when agreed upon by the fire department).
- 6) Next to required ventilation rate there also is a requirement on the velocity by which the air flows. This can be seen in de table depicted below.

In case a CFD-simulation has to be performed this has the intension to show that the sight length is higher than 30 meters from 11 minutes after the start of the fire. The CFD-simulation should also show that firemen can reach the fire in the time span of 10 to 20 minutes after the start of the fire.

Table 3: Required ventilation amount according to the Rotterdam practical guideline

Surface area	Ventilation amount
$\leq 1000 \text{ m}^2$	According to Dutch building code afd. 3.10. The required ventilation capacity is depicted for the different functions a building can have.
$> 1000 \leq 2500 \text{ m}^2$	10 times per hour with minimal velocity of $1.5 \text{ [m}^1\text{s}^{-1}\text{]}$
$> 2500 \leq 5000 \text{ m}^2$	10 times per hour with CFD simulation and minimal velocity of $1.5 \text{ [m}^1\text{s}^{-1}\text{]}$
$> 5000 \text{ m}^2$	CFD-simulation and minimal velocity of $1.5 \text{ [m}^1\text{s}^{-1}\text{]}$

## 2.5 Existing guidelines in practice

The existing guidelines meant to show the equivalence of the fire-safety level as intended by the performance requirement in the building code, are with exception of the NEN2443 meant for mechanically ventilated car-parks. As a result of this only the NEN2443 is considered by consulting agencies when assessing the fire-safety level of semi-open car parks. Therefore in practice there aren't CFD-simulations required in the design of a semi-open car park (if not asked for by the fire department) and even if the conditions on the geometry aren't met, it is still possible to show equivalence by showing that the natural ventilation is at least  $3 \text{ [dm}^3\text{/sm}^2\text{]}$  or the amount of air that can be found by using the equation in NEN2443. It has to be noticed however that the latter is based on the normal CO production of a car with a running engine. It is therefore questionable if this ventilation amount is also valid for a fire situation.



## 2.6 Comparison with international guidelines

When the Dutch NEN2443 is compared to international guidelines displayed in Table 9 [30] it can be observed that the statement that 1/3 of the car park façade is open is a requirement which can also be found in Belgium, Germany and Norway. Moreover, the other requirement in the Netherlands that each open façade has to have an open area of at least 2.5% of the surface area of the floor is comparable to the guideline in Great Britain, since at least two façades have to be open in the Netherlands which therefore is in line with the 5% open façade in Great Britain. It can also be noticed that Austria and Italy have a requirement for the total surface area of the complete building which is higher than the requirements in the other observed countries, this would lead to a larger open area for the building as a whole, however the open area per floor can potentially be lower than is the case in the Netherlands. The latter statement is certainly true for countries for which the open area per floor can be lower than 33%.

Table 4. Comparison between international guidelines, based on [30].

Country	Minimal percentage open of facade			Maximum Distance between open façades	Maximum height
	Of total facade per floor	Of total facade surface	Of floor area		
Austria	25 %	50%	-	70 [m]	8 [floors]
Belgium	33 %	-	-	-	10 [m]
Germany	33 %	-	-	70 [m]	22 [m]
Finland	30 %	-	-	-	8 [floors]
Great Britain	-	-	5 %	90 [m]	15 [m]
Italy	-	60 %	-	-	-
The Netherlands	33 %	-	2.5 %	54 [m]	20 [m]
Norway	33 %	-	-	-	16 [m]
Switzerland	25 %	-	-	70 [m]	-
United states of America	20 %	variable	-	80 [m]	23 [m]

) At least one of these conditions, the 2.5% must be met for each open facade.

### 3

## Objective

The guideline which is most often used for semi-open naturally ventilated car parks is mainly based on the amount of natural ventilation instead of the heat and smoke removal in case of fire. Since it is unknown if this will provide a fire safe situation in all conditions, an assessment of the fire-safety of semi-open car parks is made. This assessment will be based on the safety criteria discussed in the previous paragraph and will include the influences of: the façade opening area, wind effects, location of open area, a balustrade and eventually structural beams. This is done in order to provide an answer to the following research question:

*"To what extent is there a risk in the safe deployment of the firebrigade during a car fire in a semi-open car park, when the amount of natural ventilation is in line with the conditions as stated in current Dutch guidelines, and when wind-effects as well as potentially worst-case scenarios are taken into account"*

In order to provide an answer to the research question the following sub questions will be answered as well:

- What are the general car park dimensions in the Netherlands?
- Does the influence of wind provide a higher safety level in all cases when compared to a situation without wind?
- Does the distribution and location of the opening area in the façade of the car park have a significant influence on the fire safety level?
- Have structural beams placed at ceiling height a significant influence on the fire safety level?
- Does the presence of a balustrade affect the fire safety level significantly compared to a situation without a balustrade?

## 4 Method

### 4.1 Plenary approach

The following strategy is followed in order to conduct the study to the heat and smoke removal of semi-open car parks. First an identification of the Dutch regulation is made, it is analyzed if, and where potential risks in the existing regulation can be found. The next step is an identification of the most common semi-open car parks and their dimensions. Subsequently, Computational Fluid Dynamics (CFD) simulations are performed of the cases that are considered as potential hazardous or the worst case possible within the regulation. These CFD simulations need to be tested on their reliability before using them, for which a validation of the CFD simulations is made. The flow field in the case-study for the validation has to be comparable to the flow-field in a semi-open car park, which was found in a performed study of a 1.5 [MW] fire in a 88 meter long corridor. The validated CFD-simulations of the worst case situations (which are represented by 7 different variants) are assessed on the temperature and sight length safety criteria as discussed in §2.2.2 which are:

- 1) A maximum temperature at 1.8 [m] height of 100 [°C].
- 2) A maximum temperature at 2.3 [m] height of 270 [°C].
- 3) A minimal sight length of 30 [m].

As a result of this it can be analysed if it is possible that unsafe designs of semi-open car parks can be made that still satisfy the guideline. The key elements of this approach will be described in this paragraph.

### 4.2 Identification of general semi-open car park dimensions

In order to implement the discussed CFD-simulations it is necessary to perform a case-study to the basic general dimensions of semi-open car parks. This is done by the combination of bird eye images pinpointed on semi-open car parks in the Netherlands and distance determination tools based on satellite maps. By the use of a certain sample size in performing this method it can be determined which dimensions are most general for semi-open car parks in the Netherlands. The spot check size is determined by using the following relations [31].

$$N = p \cdot w \cdot \left(\frac{z}{e}\right)^2 \quad (8)$$

$$N' = \frac{N}{1 + \frac{N}{n_{pop}}} \quad (9)$$

In which:

N	=	Minimal sample size [-]
p	=	percentage of specified category [-]
w	=	percentage of non-specified category [-]
z	=	z-value at the desired reliability (99%, z=2,57) [-]
E	=	required margin of error (15%) [%]
$n_{pop}$	=	magnitude of population (1012) [-]
N'	=	corrected minimal spot check size for relative small populations [-]

By the use of a sample size of 75 car parks general dimensions for semi-open car parks in the Netherlands have been determined. The obtained a reliability of 99% and margin of 15% is calculated by the implementation of the equations discussed in 54.2. In appendix 2 an overview of the semi-open car parks of the spot check is shown. Fig. 9 and Fig. 10 summarizes the distribution of car parks towards the length (interval 10 [m]) and width (interval 5[m]) respectively.

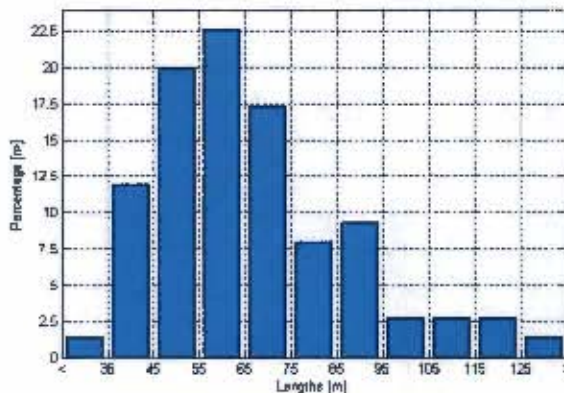


Fig. 9. Distribution of lengths of different car parks

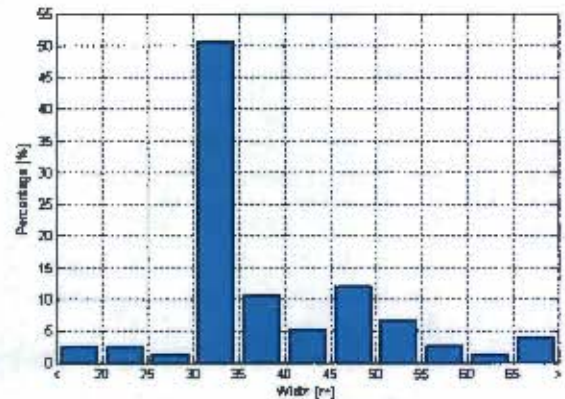


Fig. 10. Distribution of widths of different car parks

The length of a carpark which is most commonly found is between 55 and 65 meters. This is used in the simulation variants. For the width of the car park a high occurrence between 30 and 35 meters is found. The reason for this is that in most of the car parks four rows of parkingplaces are divided by two driving lanes. This is illustrated in Fig. 11 where the parking places are sketched using blue rectangles and the driving lanes are indicated by two arrows.

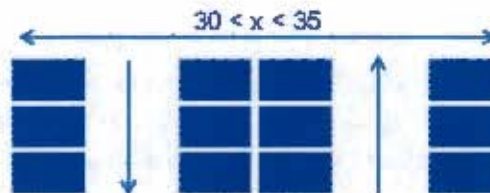


Fig. 11. Schematic representation of car park width

### 4.3 Basic principles of Computational fluid dynamics

In this chapter a brief introduction of the basic principles of computational fluid dynamics (CFD) will be provided, which is mainly meant as explanation for definitions applied in of this report. Moreover only the aspects on which a decision has to be made for the cause of this research will be discussed.

#### 4.3.1 Computational fluid dynamics in general

CFD is solving fluid flow numerically. This is done by an iterating process over finite volumes for which the partial differential Navier Stokes equations are implemented into a solver. Different solvers are available, most familiar are: JASMINE, FDS, SOFIE, PHOENICS, CFX and FLUENT. It is theoretically possible to solve the Navier Stokes equations completely by the use of direct numerical simulation (DNS), in practice however this is very time-consuming and will require huge

computational resources [32]. Moreover it's only used for very simple geometries for this reason. Another approach is to predict the flow field by large eddy simulation (LES). In this method only the large eddies are solved directly whereas the small ones are modeled using a turbulence model which takes into account the "effect" of the small eddies. This doesn't provide an exact solution, however it's less time consuming than direct numerical simulation. It should be noticed that this approach would still demand an extensive amount of finite volumes if a greater accuracy has to be obtained then is the case for the implementation of the Reynolds Averaging Navier Stokes (RANS) method. In this method the averaged Navier Stokes equations are solved, meaning that only the mean flow is solved and all eddies are modeled using a turbulence model. This approach isn't exact but it is generally applicable [33]. For this research the decision is made to assess if by the use of RANS reliable results can be obtained. If this isn't the case, then LES is the method which can be used.

### 4.3.2 Turbulence models

As discussed in the previous chapter turbulence models are needed for the implementation of RANS (and LES). The turbulence models discussed in this chapter are the standard  $\kappa$ - $\epsilon$  model, the standard  $\kappa$ - $\omega$  model and the Reynolds stress model. Which is just a fraction of the 16 different models which are available in Fluent [33], however the models discussed here are most commonly used.

#### Standard $\kappa$ - $\epsilon$ model

This is the turbulence model which is mostly used by technical consulting companies, moreover it is known that the model provides relative reliable results in a broad variety of use [33] (which is in combination with the relatively short CPU time the reason that this model is used most often). The model is half-empiric and based on a transport equation for the turbulent kinetic energy ( $\kappa$ ) and the dissipation velocity of this energy ( $\epsilon$ ). The transport equations for the turbulent kinetic energy are based on exact (analytically determined) equations, whereas the dissipation of turbulent energy does show significant differences with the mathematically determined exact solution (this because it's the empiric part of the model). The  $\kappa$  and  $\epsilon$  can be seen as a source and a sink of turbulent energy, which are a function of the velocity gradients. When large velocity gradients do exist,  $\kappa$  and  $\epsilon$  will also be larger (and vice versa). It should be noticed that the model is created with a completely isotropic turbulent flow in mind, in which molecular effects are negligible. The model should therefore only be used in these kind of fluid flows [34]

#### Standard $\kappa$ - $\omega$ model

This model does in comparison with the standard  $\kappa$ - $\epsilon$  model also determine the transport equations for the turbulent kinetic energy and the dissipation velocity of this energy. The difference can be found in the fact that the transport equations and parameters which are used are mainly meant for the determination of fluid flows near walls [33] (in the outer layer). This model could potentially provide quite reliable results because of the relatively low height in comparison to the length (large surface area of walls).

#### Reynolds stress model

This is the most detailed RANS model available in Fluent, in the creation of this model it isn't assumed that the turbulence is isotropic. Therefore this is solved by additional transport equations for each direction, moreover also the turbulent length scale is solved by the separate transport equations. Eventually this results in 7 extra transport equations (for a 3 dimensional situation)

which have to be solved for each node. For this reason the CPU time will increase when this model is used.

It is expected that this model will provide better results in case the eddies have a preferred direction. Which is for example the case in spiral shaped eddies. However it should be noticed that the implementation of this model would not result in more reliable results for all cases [33][34].

### 4.3.3 Wall treatment

The turbulence models have their utilization in the core of a room, that is to say fluent flows relatively distant from walls and other obstacles. It is therefore necessary to implement a method which can calculate the fluent flows close to walls. The later is called the wall treatment, which will be explained in this paragraph.

The flow nearby walls (the inner layer) can be subdivided in three different layers [33][34], namely:

- Viscous sub-layer or linear sub-layer
- Buffer zone
- Log-law layer

In the layer closest to the wall (the viscous sub-layer) the flow can be considered as almost laminar. In this layer the molecular viscosity plays a dominant role in the velocity and heat- and mass transport. The layer most remote from the wall but inside the inner layer is called the log-law layer, in this layer turbulence plays the most dominant role in the determination of the above mentioned parameters. The layer between these layers is called the buffer zone, in which the two mentioned effects have a comparable influence.

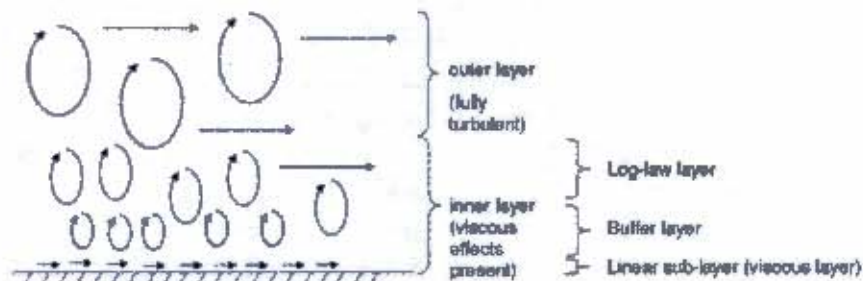


Fig. 12. Schematic representation of layers nearby walls [32].

To determine the flow nearby a wall or obstacle it is necessary to asses in which layer the first cell near the wall is located. To determine this, the  $Y^+$  value can be used. This value is also called the dimensionless wall distance, and is calculated in with following equation:

$$Y^+ = \frac{\rho \cdot y \cdot \sqrt{\frac{\tau_w}{\rho}}}{\mu} \quad (10)$$

In which:

- $Y^+$  =  $Y$ -plus value or dimensionless wall distance [-]
- $\rho$  = Density of fluid [ $\text{kg}^1\text{m}^{-3}$ ]
- $y$  = Distance of first node to wall [m]
- $\tau_w$  = Shear stress in first node from wall [ $\text{N}^1\text{m}^{-2}$ ]
- $\mu$  = Dynamic viscosity [ $\text{kg}^1\text{m}^{-1}\text{s}^{-1}$ ]

Fig. 13 shows that as a function of  $Y^+$  the  $U^+$  velocity profile can be calculated for the viscous sub layer or the log law layer. In the viscous sub layer the velocity profile can be determined cause here the statement that  $u^+=y^+$ , where  $u^+$  is the dimensionless velocity appears to be valid. However implementing this method would result in significant small cells near the boundaries, which in case of the relatively large dimensions of a car park would result in an extensive amount of nodes. This is undesirable because of the large CPU-time in which this would result. Therefore it is for this case more desirable to create first cell dimensions which result in a  $Y^+$  value that makes the calculation of the velocity profile in de log law layer possible. As the name of this layer indicates the velocity profile in this area can be expressed by a logarithmic equation, namely  $u^+=\kappa^{-1}\ln(Y^+)+B$ . The  $Y^+$  value to determine the velocity profile in this layer has to be between 30 and 300 (in Fluent) [33]. The jargon implemented in the CFD to refer to this method is the use of wall functions. This name will be used in this report.

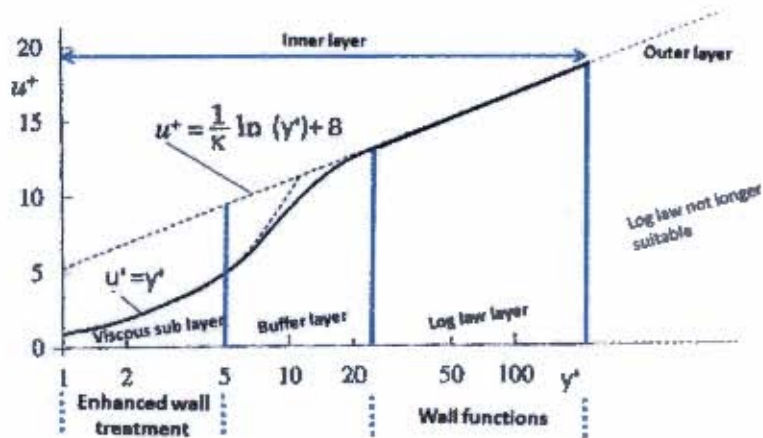


Fig. 13. Determination of  $U^+$  as a function of  $Y^+$  (original graph from [35] which is altered for this report).

#### 4.3.4 Wind pressure and turbulence intensity

In a case of the absence of wind the only driving force for the movement of heat and smoke in a semi-open car park will be the buoyancy forces due to the differences in air densities created by the high temperature of a fire. However since a semi-open car park can be effected by wind also the created impulses of the wind on the smoke layer can potentially play a significant role in the heat and smoke removal in semi-open car parks. To obtain insight in the influence of wind on a car fire, different wind velocities will be created on the facade of the car-park model. This will be done by determining the dynamic pressures belonging to certain velocities throughout the car park by the use of Bernoulli's equation. To determine the turbulence intensities which are likely to belong to the specified velocities it is necessary to take the landscape description and observed height into account. For the landscape description the revised davenport roughness classification is used [36]

which can be seen in Table 5. Since a car park can be found near large shopping area's or near industry and offices, it is assumed that the appropriate aerodynamic roughness length is equal to a "closed" situation.

**Table 5. Revised davenport roughness classification [46]**

$Y_0$ [m]	Landscape description
0.0002 "sea"	Open sea or lake (irrespective of the wave size), tidal flat, snow-covered flat plain, featureless desert, tarmac and concrete, with a free fetch of several kilometers.
0.005 "Smooth"	Featureless land surface without any noticeable obstacles and with negligible vegetation; e.g. beaches, pack ice without large ridges, morass, and snow-covered or fallow open country.
0.03 "Open"	Level country with low vegetation (e.g. grass) and isolated obstacles with separations of at least 50 obstacle heights; e.g. grazing land without windbreaks, heather, moor and tundra, runway area of airports.
0.10 "Roughly open"	Cultivated area with regular cover of low crops, or moderately open country with occasional obstacles (e.g. low hedges, single rows of trees, isolated farms) at relative horizontal distances of at least 20 obstacle heights.
0.25 "Rough"	Recently-developed "young" landscape with high crops or crops of varying height, and scattered obstacles (e.g. dense shelterbelts, vineyards) at relative distances of about 15 obstacle heights.
0.5 "Very rough"	"Old" cultivated landscape with many rather large obstacle groups (large farms, clumps of forest) separated by open spaces of about 10 obstacle heights. Also low large vegetation with small interspaces, such as bush land, orchards, young densely-planted forest.
1.0 "Closed"	Landscape totally and quite regularly covered with similar-size large obstacles, with open spaces comparable to the obstacle heights; e.g., mature regular forests, homogeneous cities or villages.
>2 "Chaotic"	Centers of large towns with mixture of low-rise and high-rise buildings. Also irregular large forests with many clearings.

A second assumption that is made is that a higher turbulence intensity will result in a higher mixing factor of the incoming fresh air with the air inside a car park which has a high temperature and smoke concentration. As a result of the high smoke potential of a car fire the higher mixing will result in a larger surface area where the sight length will be minimal (in contrast to the a case with a lower amount of mixing, in which the heat and smoke removal as a result of the wind pressure is assumed to be higher). In precedence of this assumption it is determined that the higher turbulence intensity will occur near ground level. The relation between the turbulence intensity and the height from ground level is shown in Fig. 14 where measurements are presented which have been performed in a wind tunnel [37]. The velocity profile can be expressed with a power-law expression (with an exponent equal to 0.15) and the turbulence intensity (which is calculated by dividing the standard deviation of the measured air velocities by the average air velocity at a certain height) is inversely proportional to the height. It can therefore be concluded that the highest turbulence intensity can be found near to the ground level in a real situation as well.



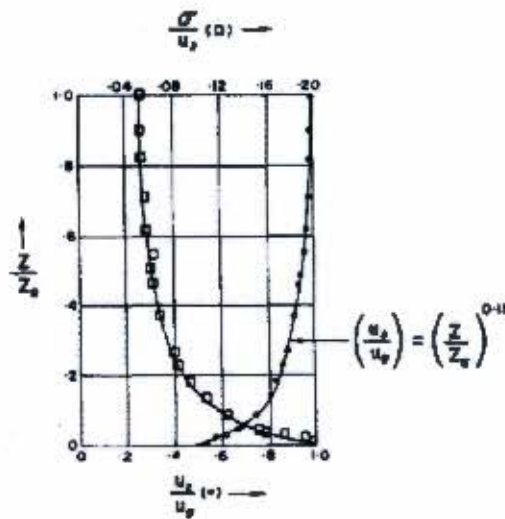


Fig. 14. Experimental wind velocity and turbulence intensity profiles [47]

To calculate the turbulent dissipation velocity and turbulent kinetic energy at a certain air velocity, height and landscape description the equations displayed below can be used [38][39]. To make the implementation possible, it is found that for a aerodynamic roughness length of 1.0 ("closed") the turbulent intensity ( $I_u$ ) is about 40% at pedestrian height [40].

$$U(y) = \frac{U_{ABL}^*}{\kappa} \cdot \ln\left(\frac{y + y_0}{y_0}\right) \quad (11)$$

$$\varepsilon(y) = \frac{U_{ABL}^{*3}}{\kappa(y + y_0)} \quad (12)$$

$$k(y) = \frac{3}{2} \cdot (I_u \cdot U(y))^2 \quad (13)$$

In which:

- $U(y)$  = Velocity at height  $y$  [ $m^1s^{-1}$ ]
- $U_{ABL}^*$  = Friction velocity [ $m^1s^{-1}$ ]
- $\kappa$  = Von Karman constant (0.42) [-]
- $y$  = Vertical coordinate [m]
- $y_0$  = Aerodynamic roughness length [m]
- $\varepsilon(y)$  = Turbulent dissipation velocity at height  $y$  [ $m^2s^{-3}$ ]
- $k(y)$  = Turbulent kinetic energy [ $m^2s^{-2}$ ]
- $I_u$  = Turbulent intensity [%]

Out of these equations can be converted that in the case that is known which dynamic wind pressure on the surface of a car park building will lead to an air velocity through the building that is interesting for this investigation, the following relation can be used to calculate the turbulent dissipation velocity and turbulent kinetic energy (in these equations also Bernoulli's equation and the relation  $p_s = C_p \cdot p_v$  [41] which gives the relation between the wind pressure on the building surface ( $p_s$ ) and the outdoor atmospheric pressure at the same level in an undisturbed wind approaching the building ( $p_v$ ) are implemented).

$$\varepsilon(y) = \frac{\kappa^2 \cdot \left( \frac{2 \cdot p_s(y)}{C_p \cdot \rho_a} \right)^{\frac{3}{2}}}{\ln\left(\frac{y}{y_0} + 1\right)^3 \cdot (y + y_0)} \quad (14)$$

$$k(y) = \frac{3}{2} \cdot \left( I_u \cdot \frac{2 \cdot p_s(y)}{C_p \cdot \rho_a} \right)^2 \quad (15)$$

In which:

- $p_s(y)$  = Dynamic pressure at height  $y$  [pa]
- $C_p$  = Wind induced pressure coefficient [-]
- $\rho_a$  = Ambient outdoor air density [ $\text{kg}^1\text{m}^{-3}$ ]

The wind induced pressure coefficient is dependent of the direction of the wind. In the table displayed below the wind induced pressure coefficient can be seen for different wind directions compared to the normal of the facade, for a rectangular shaped building with a flat roof of which the widest facade is three times wider than the smallest one [41]. Out of this table can be concluded that for a case in which the wind flows strait into the car park building, the  $C_p$  will be equal to 0.9.

Table 6. Wind Induced pressure coefficient for different angles [41]

Wind direction (compared to normal on facade)	$C_{p, in}$ [-]	$C_{p, out}$ [-]	$C_p$ [-] ( $C_{p, in} - C_{p, out}$ )
0	0.6	-0.30	0.90
30	0.5	-0.31	0.81
60	0.01	-0.53	0.54
90	-0.65	-0.65	0.00

With the information described above it is possible to determine the turbulent dissipation velocity and turbulent kinetic energy at a certain wind pressure used in a CFD simulation.

## 4.4 Basic principles of fire and fire-modelling

In this paragraph some basic principles of fire and fire-modelling which are used in the CFD-simulations for both the case-study and the simulation of the different variants will be discussed.

### 4.4.1 Pool-fires

As discussed in §4.1 a 1.5 [MW] diesel pool fire was created in the corridor of the case-study. In order to provide more insight in the dimensions of this fire a study is performed for a proper implementation into the CFD-model. It is described in the case study [42] that eight diesel pans were used to create the fire. Therefore it is determined which height and diameter one pan fire of 0.1875 [MW] would have. In order to obtain this, it is calculated which regression rate a diesel pan fire would have with different pan diameters. The equation used for this is:

$$RR(d) = \frac{4 \cdot P}{\pi \cdot \rho \cdot \sigma \cdot d^2} \cdot 60,000 \quad (16)$$

In which:

- RR = Regression rate [ $\text{mm}^2 \text{min}^{-1}$ ]
- P = Power of fire [W]
- $\rho$  = Density of liquid [ $\text{kg}^3 \text{m}^{-3}$ ]
- d = Diameter of pan fire [m]
- $\sigma$  = High heating value [ $\text{J}^1 \text{kg}^{-1}$ ]

The result of this equation for diesel as a liquid is plotted in Fig. 16, In the same graph the regression rates are displayed as a function of the diameter for different liquids. Out of the graph can be obtained that one pan will have a diameter of roughly 46 [cm] (this is the point where the regression rate of diesel oil intersects the 0.1875 [MW] fire line). By the implementation of the results in the graph displayed in Fig. 15 it can be obtained that the flame height of the fire is about 1.2 [m]. Therefore the total volume of the fire created is estimated to be roughly 1.7 [ $\text{m}^3$ ], which is the fire volume that is used in the CFD simulation of the case study.

### 4.4.2 Car-fires

Out of the background information discussed in §2.2 it appeared that it's unlikely that there are more than three cars on fire during a fire in a car park. Therefore three different heat sources are used for the implementation of these fires into the CFD-model. Moreover it is assumed that the second car will burn 10 minutes after the ignition of the first car and the third car will burn 5 minutes after the second car starts burning, this is in line with the fire curve used in the guideline for mechanically ventilated car parks which is currently in development [44]. The fire curve of one burning car is based on measurements performed by TNO (Toegepast Natuurwetenschappelijk Onderzoek) which are visible in Fig. 17. Moreover it is assumed that it takes 5 minutes from the start of the fire before it is detected, after which the fire brigade will need 10 minutes to reach the location of the car park and 5 more minutes to prepare their equipment on location and to reach the fire. Meaning that 20 minutes after the start of the fire, the firemen can have water on the fire

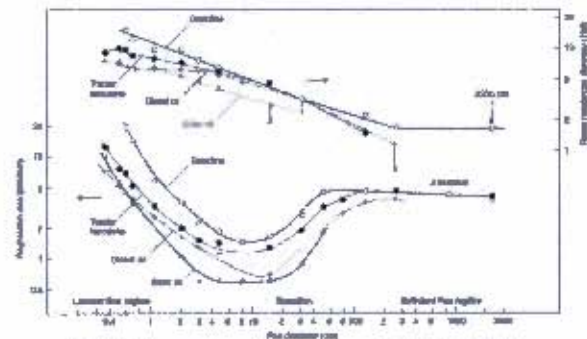


Fig. 15. Regression rate and flame height data [43]

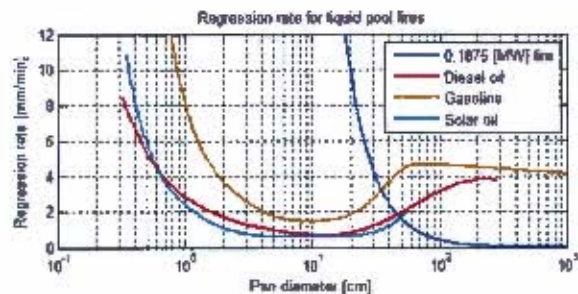


Fig. 16. Regression rate for liquid pool fires and plotted 0.1875 MW fire

as long as they can reach the fire in a safe manner. Meaning that the CFD-simulations will be done till this point to assess the situation on its safety using the criteria discussed in §2.2.2. For the fire curve of three combined car fires visible in Fig. 18 it can be observed that the heat release at this point is roughly 9 [MW].

For the smoke a production of 400 [m<sup>2</sup>kg<sup>-2</sup>] burned fuel is assumed with a heat of combustion of the burning car material of 25 [MJ<sup>1</sup>kg<sup>-1</sup>]. The cars are simulated by a solid block of 1.0 x 4.2 x 1.7 m (h x l x w) above which a volume is created with the same size where the heat is released. The distance between the car is based on the minimal width that a parking place must have on basis of the requirements in NEN2443 [25]. Therefore based on a 1.7 [m] width car the distance between the cars is set to 0.65 [m] (minimal parking place width is 2.35 [m]).

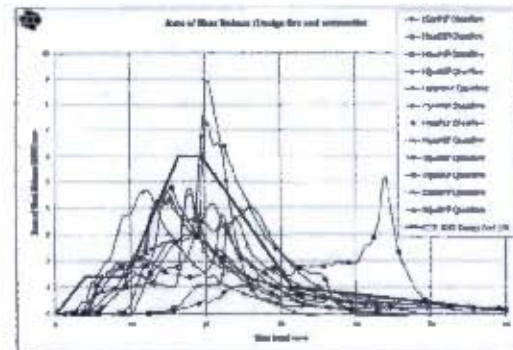


Fig. 17. Fire scenarios as measured by TNO [45]

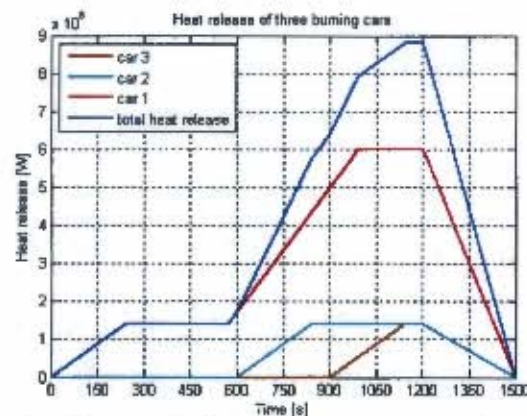


Fig. 18. Fire curve for the case that three cars are one fire

#### 4.4.3 Sight length through smoke

The normal definition of smoke refers to a combination of solid, liquid and gas residue of combustion and the air in which these products are mixed [46]. In mathematical models this definition isn't practical, most often the concentration of combustion products is used, expressed in kg<sup>1</sup>m<sup>-3</sup>. The smoke production is important because of its hindrance in case of evacuation of people. This hindrance is caused by the toxicity of the smoke and reduction of the sight length. The sight length is dependent on several factors like [46]:

- Contrast between the observed object and background
- The degree of lighting of the object
- The color of the smoke
- Other light sources of which the light is diffused
- Physiological effects of smoke, like eye irritation
- The power of observation which can be influenced by fire related stress

For a more general application most aspects discussed above aren't taken into account and general rules of thumb are used. These rules are based on the optical smoke density which can be measured by the decrease of a light source over a certain distance. Out of this optical smoke density the sight length can be determined on bases of studies which are performed with human subjects in the years 1960 to 1980.

The following equations are a result of these studies:

$$SL_{tr} = \frac{1}{OSD} \quad (17)$$

$$SL_l = \frac{2.5}{OSD} \quad (18)$$

$$SL_{prac} = \frac{1.3}{OSD} \quad (19)$$

In which:

- $SL_{tr}$  = Sight length towards light reflecting object [m]
- $SL_l$  = Sight length towards a light source [m]
- $SL_{prac}$  = Sight length defined by the Dutch practical guideline [m]
- $OSD$  = Optical smoke density [ $m^{-1}$ ]

In the calculation of the optical smoke density it is important to take the thermal power, ventilation rate and the material that is burning into account. As the smoke production is linked to the heat release of the fire. Moreover the ventilation rate is important because a lack of oxygen for the fire would in most cases results in larger production of smoke due to the incomplete burning. For assessing the smoke production of a specific material standardized testing methods exist. For example a static test in which all the burned products of a specific volume of the material are collected and then mixed homogeneous, though this volume the light intensity decrease is determined which is expressed in  $m^2kg^{-1}$  ( $m^{-1}m^3kg^{-1}$ ). The smoke production can differ significantly between different materials. For the most generally used materials the value for the smoke production is between 200 and 400 [ $m^2kg^{-1}$ ].

In case of a car fire the smoke production can be larger than 400 [ $m^2kg^{-1}$ ] for short moments especially for modern cars in which a significant amount of plastics are present. However because this are only peaks in the total duration of a car fire, it is realistic to set the smoke production on an average of 400 [ $m^2kg^{-1}$ ] over the total time span of the fire [46]. To link this smoke production to the heat release of a car fire in literature is found that the average heat production of a kilogram "burned car" will deliver about 25 [ $MJ^1kg^{-1}$ ] of heat. Out of which can be determined that the smoke production is about 16 [ $m^2MJ^{-1}$ ] which is implemented in the simulation.

#### 4.4.4 Weighted sum of gray gasses model

Considering the irradiative heat transfer of smoke the soot concentration plays a significant role. Heat is absorbed by these soot particles and subsequently transmitted by radiation, eventually equilibrium between emission and absorption occurs. Next to the soot particles other components in smoke like carbon dioxide and vaporized water should be considered in the irradiative heat transfer. These gases absorb and emit energy at specific wave numbers which is described by quantum physics. For this reason approximation models exist which describe the radiative properties of gases and smoke. In this research the weighted sum of grey gasses model (WSGGM) is used. In essence this model states that the total emissivity and absorptivity which is a function of temperature and smoke density can be represented by the sum of a gray gas emissivity weighted with a temperature dependant factor [47].

#### 4.4.5 Thermal capacity of walls

Considering the boundary conditions of the walls different approaches can be used, in the CFD-model a one dimensional heat transfer model has been used. For the proper implementation of the walls the thermal capacity of these walls is taken into account. Therefore temperature dependant properties of the wall material are taken into account. In Fig. 19 to Fig. 22 the properties can be seen as a function of the temperature. It is visible that both gypsum and concrete have a high peak in the specific heat around 100 [°C] which is a result of the moisture content in the material. Moreover it can be observed that where the thermal conductivity of gypsum increases with temperature, for concrete it decreases.

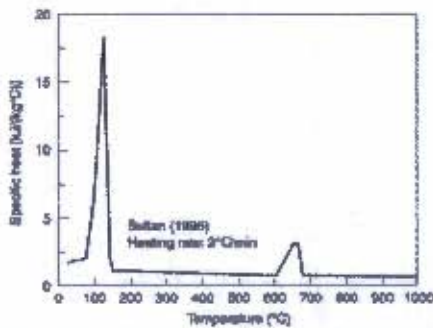


Fig. 19. Specific heat of gypsum board as a function of temperature [48]

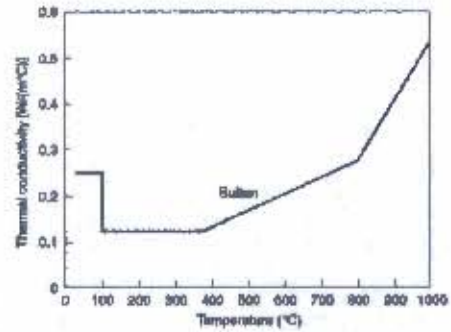


Fig. 20. Thermal conductivity of gypsum board as a function of temperature [48]

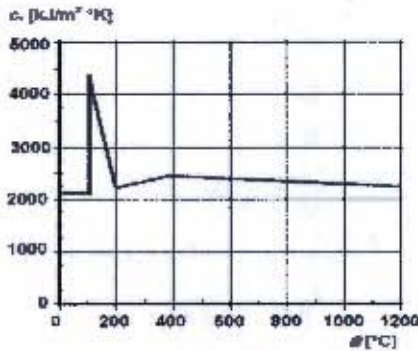


Fig. 21. Volumetric specific heat as a function of temperature of siliceous concrete with a 3% moisture content [49]

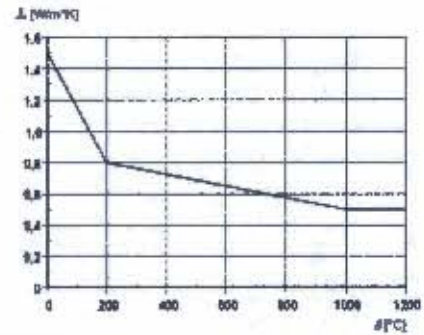


Fig. 22. Thermal conductivity of siliceous aggregate concrete [49]

## 4.5 Case study for validation

### 4.5.1 Description of case study

In the approach that will be used for the assessment of the fire safety of a semi-open car park the role of Computational Fluid Dynamics (CFD) simulation is of high importance. In order to make sure that the results of these simulations will provide reliable results, a validation of the CFD-model is performed. This validation is done by the use of a case study as described in the following paper: Full-scale burning tests on studying smoke temperature and velocity along a corridor [42]. This paper provides the experiments that were conducted in an underground corridor measuring 88 m long, 8 m wide and 2.65 m high of which one end was closed. The sidewalls of the corridor were made of concrete and the ceiling was made of gypsum. At the closed end a diesel pool fire was created with a maximum heat release of 1.5 MW. The temperature underneath the ceiling was measured using a total of 49 thermocouples and 8 thermal resistors along the length of the corridor. In Fig. 23 depicted below an overview of the experimental layout can be seen.

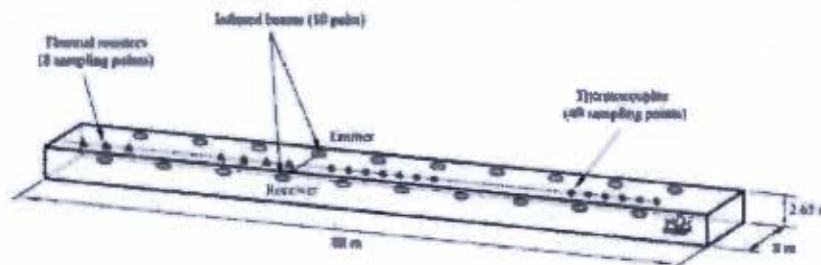


Fig. 23. Schematical overview of experimental layout.

CFD-simulations are performed under the same conditions as was the case during the experiments, subsequently the results are compared. A comparison is made on the temperatures underneath the ceiling over the time span of the fire and the maximum temperatures that could be found over the length of the corridor. These two results of the measurements are depicted in the figures below. In Fig. 24 temperature as a function of time is shown for several positions from the fire. In Fig. 25 the maximum temperature measured during the time span of the fire can be seen, where on the horizontal axes the distance from the fire, and on the vertical axes the maximum temperature is shown.

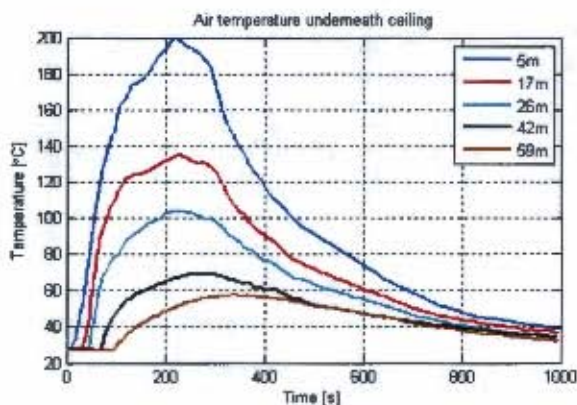


Fig. 24. Air temperature underneath ceiling.

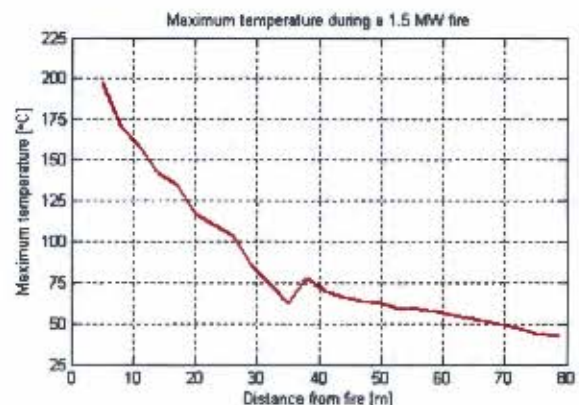


Fig. 25. Maximum temperature during a 1.5 MW fire

This case is appropriate for validation for several reasons, first of all the geometry of the corridor, has a comparable height as the height of a common car park. Moreover the geometry is straight on, without any oddities. A second reason is that the created smoke layer isn't influenced by any constrains (like jet-fans or opening) which makes it a free flooding ceiling jet which is comparable to the situation that can be found in a semi-open car park. A third reason is the created fire which is a liquid pan fire that is well defined in literature. And a last reason is that all the necessary boundary conditions to perform a CFD-simulation are known.

#### 4.5.2 Comparison of simulation and measurements

The simulation results will be compared towards two different aspects, the temperature distribution at several positions at ceiling height over the time span of the fire and the maximum temperatures that occur during the fire over the entire length of the corridor. Several boundary conditions have been tested by the

use of CFD. Fig. 26 to Fig. 28 show results obtained from three different conditions. In these graphs the time is depicted on the horizontal axes and the temperature underneath the ceiling on the vertical axes. The solid lines give the measured result; the dotted lines provide the simulation result. Fig. 26 indicates that when adiabatic boundary conditions are used this will result in predicted temperatures which are significantly higher than measured, however when the boundaries are set on the initial temperature of 27 °C the temperatures will be lower in most of the observed points. Both the methods provide quite significant errors:

- The error with an adiabatic boundary is explained by the negligence of the amount of heat which is absorbed in the walls and ceiling over the relatively short time of the fire. This results in temperatures predicted by the model that are too high.
- The error with the boundaries set on 27 °C is explained by the fact that in reality the boundaries will reach higher temperatures, resulting in a decreasing amount of heat which is transferred towards the boundaries over the time of the fire.

Therefore the third method is used which takes the thermal capacity of the walls into account. The results indicate that this model does predict the temperatures in a more accurate way. Fig. 29 shows the maximum temperatures over the entire length of the pool-fire found in the simulation compared to the measurements for this method. Where on the horizontal axes the

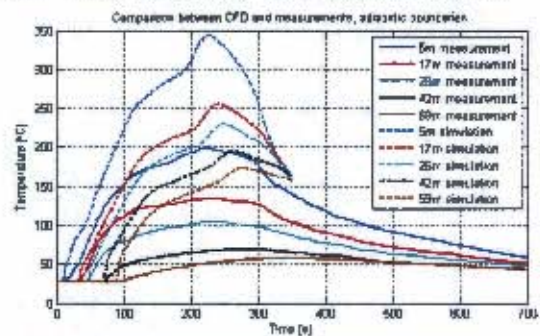


Fig. 26. Comparison between CFD and measurements, adiabatic boundaries

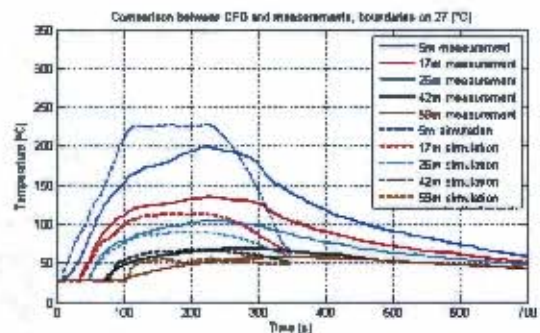


Fig. 27. Comparison between CFD and measurements, boundary on 27 °C

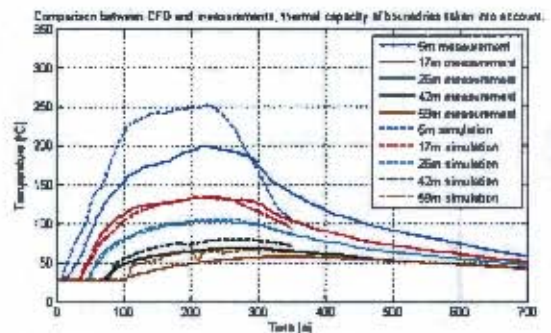


Fig. 28. Comparison between CFD and measurements, thermal capacity of boundaries taken into account



distance from the fire, and on the vertical axes the maximum temperature is expressed. From this result it is concluded that the results from the CFD-simulation and the measurement are in good agreement, and therefore that the model predicts reality in a sufficient accurate way. In addition the error defined as simulation result minus measurement results is always positive. This indicates that when an error is involved this error will always be that the temperatures are slightly higher than in reality. This assumes that the model provides a conservative result. If a result found by simulation is considered as safe, this would also be the case for reality which would probably be slightly more positive.

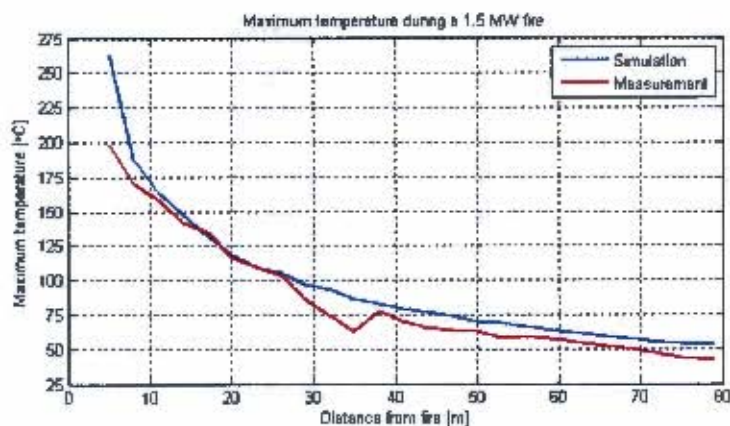


Fig. 29. Maximum temperatures underneath ceiling over the time span of the fire

Out of the results can also be observed that the model has the largest absolute error close to the fire. This error reduces with an increase in distance from the fire. In order to evaluate the simulated temperatures over the time span of the fire in more detail, the results at larger distances from the fire are assessed on their accuracy (see Fig. 30). The percentage difference (calculated with degrees Celsius) between the measurement and simulation are displayed in Fig. 31. The results show that a significant error is induced at the moment that the smoke layer reaches the observed points distances. However this error reduces over time. To provide the average error over time the Root Mean Square (RMS) is used. Which is calculated by the following integral:

$$RMS = \sqrt{\frac{1}{t} \cdot \int_0^t \left( \frac{x_{\text{cfd}} - x_{\text{measurement}}}{x_{\text{measurement}}} \cdot 100\% \right)^2 dt} \quad (20)$$

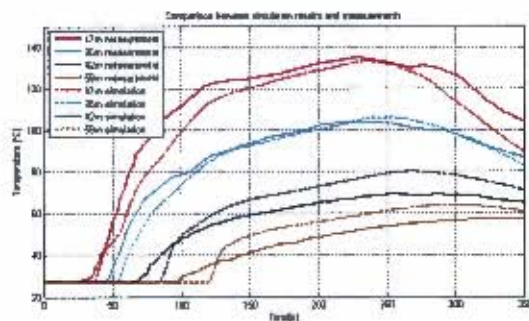


Fig. 30. Comparison between CFD and measurements in more detail



Fig. 31. Error between CFD and measurements displayed in percents

In which:

- $RMS$  = Root mean square of error [%]  
 $t$  = Time [s]  
 $X_{cfd}$  = Temperature found with CFD simulation [°C]  
 $X_{measurement}$  = Temperature found with measurements [°C]

In Fig. 32 the RMS is visible over time, eventually the average error over time at 17, 26, 42 and 59 meter are respectively 9.0%, 7.3%, 11.9% and 12.4%. At 5 meter distance from the fire which isn't displayed in the graph the average error over time is 37.8%. This large error less than approximately 10 meters from the fire is also visible in Fig. 29, therefore it is observed that the results close to the fire will be less reliable, however based on four points the maximum error based on four points the maximum error found more than 10 meters from the fire is assessed 12% over time. The average error over the four observed points was 10%, which was accomplished using the boundary conditions visible in Table 7.

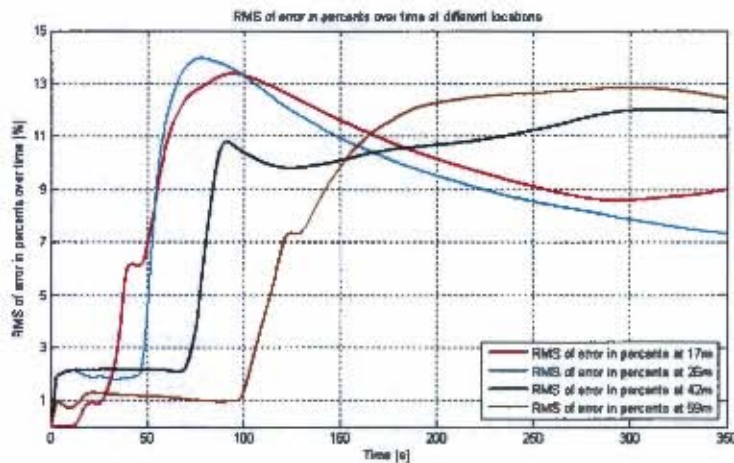


Fig. 32. Root mean square of error in percents

Table 7. Used boundary Conditions for CFD simulation of case study

Object	Used
Grid	Structured, minimal cell size 10 [cm] with maximum grow rate of 1.05. Total 98,154 nodes
Unsteady solver	time 350 [s] / $\Delta t=1$ [s]
Covergence criteria	Velocities: $10^{-4}$   Energy: $10^{-5}$   $\kappa$ : $10^{-3}$   $\epsilon$ : $10^{-3}$   DO: $10^{-4}$
Turbulence model	Standard K- $\epsilon$
Wall treatment	Standard wall functions
Radiation model	Discrete Ordinates
Walls	1D heat transfer $T(t=0)= 27[^\circ\text{C}]$ in which the thermal capacity of concrete (walls and floor) and gypsum (ceiling) are included.
Outlet	pressure outlet, $\Delta P=0$ [pa] temperature of entering air is $27[^\circ\text{C}]$ .
Heat release rate of fire	Maximum 1.5 MW, for fire curve a linear increase is assumed.
Volume fire	determined by regression rate of liquid pool fires which resulted in a fixed fire volume of 1 [m <sup>3</sup> ]
Smoke	Generation of 0.1 kg/MW
Emissivity and absorption	Weighted Sum of Gray Gases Model (WSGGM)

### 4.5.3

### Determination of simulation characteristics

In this paragraph the following CFD-model characteristics are presented: Grid sensitivity, Influence of turbulence model and the wall treatment.

#### Grid sensitivity

To determine if the results obtained are grid independent, a grid sensitivity study is performed. Several simulations have been run in which only the grid size was changed. The results have been evaluated using the same analysis as discussed in §4.5.2 where the average error over time over four points is determined. The grid size is changed leaving the first cell size near the boundaries 10[cm] in the direction of the normal on the surface, this is done to leave the influence of the y-plus value unchanged. The grid sizes are roughly doubled for each case. In Fig. 33 the different grids are visible, in this figure the detailed grid in the area around the fire (displayed in green) can be seen. Moreover it is visible that the first cells at the boundaries are left unchanged in size and the amount of nodes ranges from 28,380 to 580,635. In Fig. 34 the assessed simulation results for the different grid sizes can be seen. In this graph the number of nodes are set on the horizontal axes and the average error on the vertical axes. Out of these results can be observed the grid size influences the simulation results in a significant way. The average error differ from 10% to 26%.

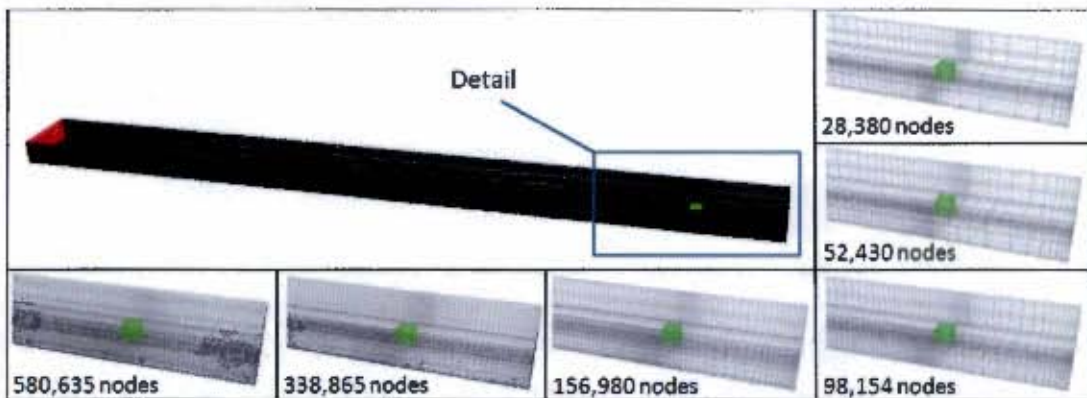


Fig. 33. The six different grid sizes which are used, the amount of nodes are visible for each case.

Moreover it can be seen that when more than 52,430 nodes are used the error differs between 10% to 15%. Since from this point the error differs no more than 5% it is assumed that a grid independent solution is obtained. The minimal grid size for this simulation is determined to be one grid refinement smaller than the first time the error was below 15% which therefore is: 98.154 nodes.

The characteristics of this grid are:

- A structured grid.
- First cell size normal on any boundary is equal to 10 [cm].
- The maximum growth rate for one cell to the adjoining one is 1.05.
- The length over which the error is observed is 59 [m], therefore it is determined that the maximum length over which the cells grow must not exceed this length. Because otherwise the stated accuracy could be different.

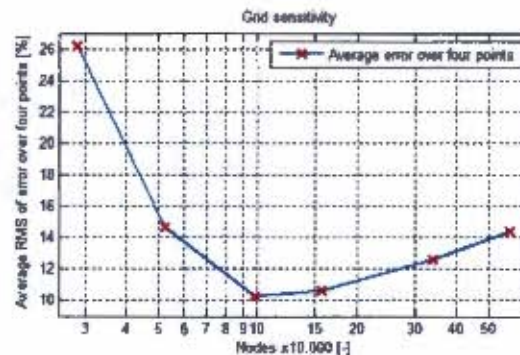


Fig. 34. Average RMS of error over four points as a function of the amount of nodes.

### Influence of turbulence model

It is demonstrated in §4.5.2 that reliable results were found when the measurement results of the case study are compared with the CFD-results. In order to determine the influence of the turbulence model, different turbulence models have been tested by. Two other turbulence models have been tested in addition to the standard  $\kappa$ - $\epsilon$  model; the standard  $\kappa$ - $\omega$  model and the Reynolds Stress model as discussed §4.3.2 The method used for the comparison is equal to the method as discussed in §4.5.2 which provides an average error over time. The results of this comparison are displayed in Fig. 35. Out of which is observed that another turbulence model isn't likely to provide better results with the use of the current grid and boundary conditions.

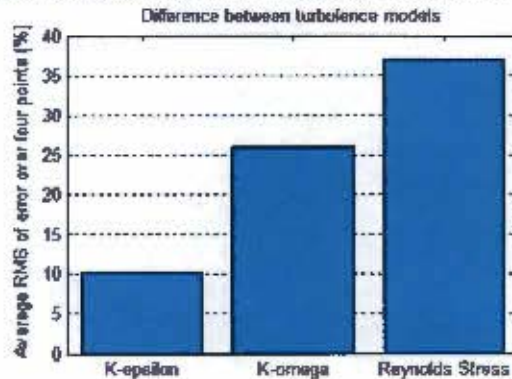


Fig. 35. Comparison on reliability by the use of different turbulence models

### Application of the wall-functions

As discussed in §4.3.3 the  $Y^+$  value needs to be between 30 and 300 in order to provide a sufficient prediction of the velocity profile nearby the boundaries. To asses if this is the case over the total time span of the fire, the  $Y^+$  value is observed over the length of the corridor for the entire time interval. Out of these results the graphs displayed in Fig. 36 and Fig. 37 have been developed. In these graphs the  $Y^+$  value is plotted as a function of time and distance from the fire in longitudinal direction. The graphs show that the  $Y^+$  value is between these values for the majority of observed points (moreover it can be seen that the value is only exceeded with approximately 17% for about 100 seconds at a location less than 10 meters from the fire).

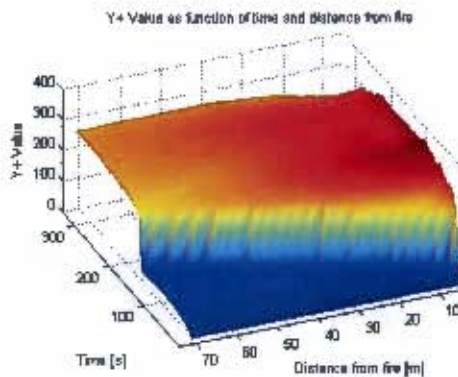


Fig. 36. Y-plus value at ceiling in a horizontal line over the length of the corridor displayed over time.

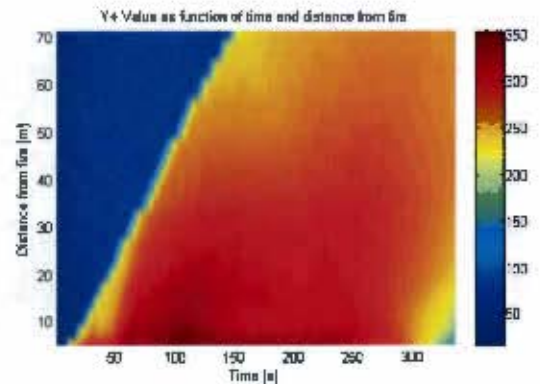


Fig. 37. Y-plus value at ceiling in a horizontal line over the length of the corridor displayed over time observed from top.

## 4.6 Transition from validation case to car park simulation

### 4.6.1 Description of transition case

The discussed validation case in §4.5 has a free flooding ceiling jet which is comparable to a case concerning a semi-open car park. However where the validation case describes a case in which the flow is mainly in one direction the case of a semi-open car park will be omnidirectional. Therefore a transition case is used in which the same fire is created as in the validation case yet with a geometry comparable to a car park. The used geometry is a result of the study on general dimensions for semi-open car parks as discussed in §4.2 and the outcome of the case study. The results of the transition case are compared to the Alpert's correlation [50] (depicted below) which gives the velocity and temperature of a free flooding ceiling jet as a function of distance from the fire, heat release of the fire, ceiling height and starting temperature.

By the use of this it is checked if the created model will also provide reliable results for a case in which the flow is multidirectional.

$$U = 0.195 \cdot \frac{(\dot{Q}/H)^{1/3}}{(r/H)^{5/6}} \quad (21)$$

$$T = 5.38 \cdot \frac{\dot{Q}^{2/3}/H^{5/3}}{(r/H)^{2/3}} + T_{\infty} \quad (22)$$

In which:

$U$	=	Velocity [ $\text{m}^1\text{s}^{-1}$ ]
$T$	=	Temperature [ $^{\circ}\text{C}$ ]
$\dot{Q}$	=	Heat release [kW]
$r$	=	Distance from fire [m]
$H$	=	Ceiling Height [m]
$T_{\infty}$	=	Starting temperature [ $^{\circ}\text{C}$ ]

### 4.6.2 Comparison of simulation and transition case

It has become clear that the CFD-simulations of the case study show results which are comparable to the results of the measurements. In this chapter the transition towards a simulation of a car park will be discussed.

#### Implementation of obtained results of case-study

As a result of the general car-park dimensions as discussed in §4.2, the dimensions of the car-park model for the transition case towards a semi-open car park are chosen to be 35 [m] x 65 [m] (width x length). For the height 2.4 [m] is used. The fire created inside the car park is similar to the pool-fire used in the case study and is placed in the middle of the car park, moreover the created grid has the same characteristics as discussed in §4.5.3. The walls are completely open (pressure outlets) which makes the comparison with the Alpert's correlation possible. This correlations is only valid for a complete omnidirectional free ceiling jet smoke layer which is created by the eliminations of walls. The applied grid can be seen in Fig. 38 where the pressure outlets are displayed in red and the fire volume in green.

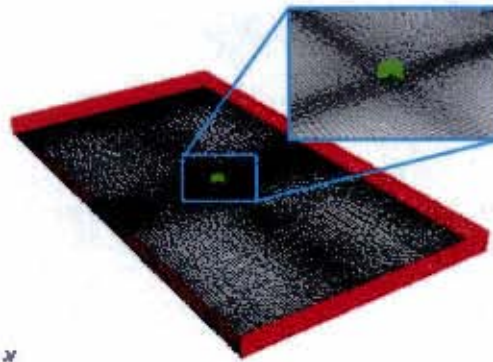


Fig. 38. Used grid (652,533 nodes) for transition case towards simulation of semi-open car park

#### Comparison with Alpert's correlations

For the comparison the velocities and temperatures 0.15 [m] underneath the ceiling are monitored in longitudinal- and perpendicular direction of the fire. These results are displayed in Fig. 39 to Fig. 42 where on the horizontal axes the distance from the fire is presented, and on the vertical axes the temperature and the velocity. In the graphs the simulation results are displayed in red and the results obtained by the Alpert's correlations in blue. It can be observed that the prediction more than two meters from the fire does show good agreement with the correlation. Therefore it is assumed that in case of an omnidirectional free ceiling jet smoke layer the CFD model also predicts the temperature and velocities in an accurate way. As a result of this it is stated that the CFD model will predict the airflow pattern inside a car park in a sufficient accurate way to allow comparison of results between different variants.

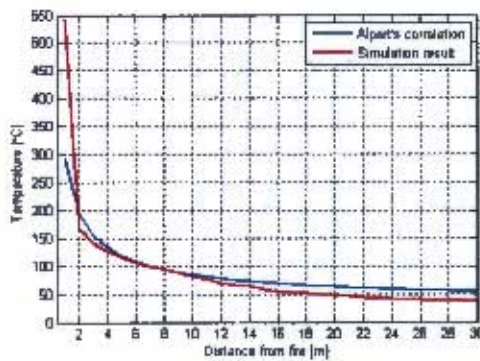


Fig. 39. Temperature x-direction

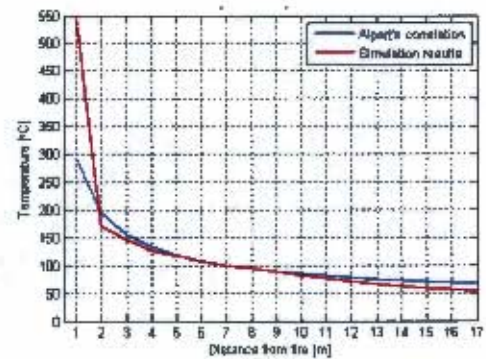


Fig. 40. Temperature y-direction

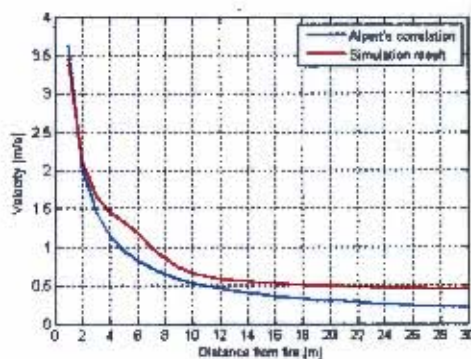


Fig. 41. Velocity x-direction

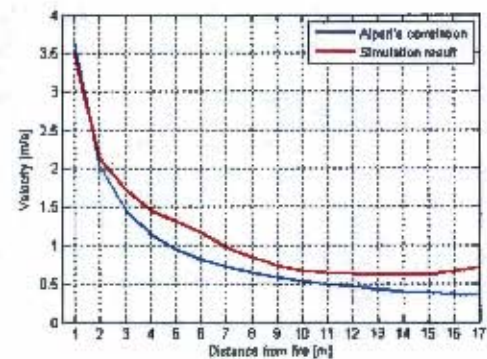


Fig. 42. Velocity y-direction

## 4.7 Set-up of simulation of semi-open car parks

It has become clear that the CFD-simulations of the transition case shows results which are comparable to the results of the Alpert's Correlation. In this chapter the results of the simulation of the car park variants will be shown.

### 4.7.1 Implementation of obtained results out of transition case

The dimensions of the car park which are obtained in §4.2 and already used §4.6 are also used for the simulation of the different variants, and are 35 [m] x 65 [m] (width x length). For the height 2.4 [m] is used. In these simulations the cars are placed on one end of the carpark, which is visible in Fig. 43 where the volumes for the heat release of these cars are displayed in green. The implementation of the cars does influence the amount of cells used, due to the expansion the volume where the heat is released (where smaller cells are used). The total amount of nodes of the simulation of variants 1 to 6 discussed in § 4.7 is 930,147 nodes. The amount of nodes for variant 7 is much larger because of the implementation of the structural beams (discussed in appendix 1) around which a grid of 10 [cm] is used, the amount of volume cells is 1,941,417.

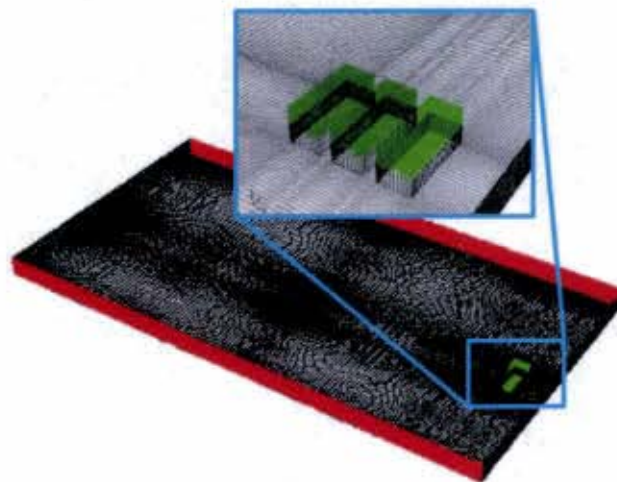
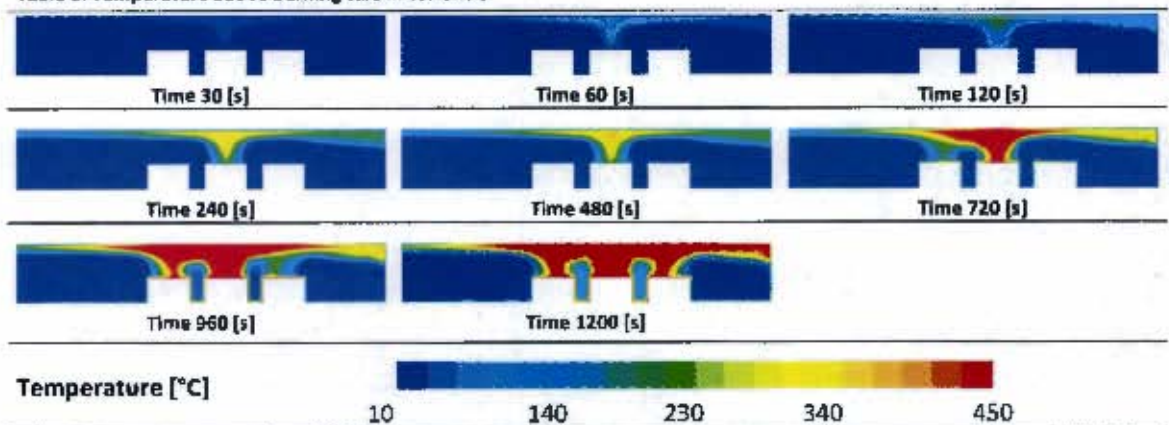


Fig. 43. Example of used grid and geometry (930,147 nodes; open walls on long sides; closed short sides; no structural bearings)

#### 4.7.2 Heat and smoke implementation check

Considering the heat generation near the cars Table 8 shows how the temperature above the cars increases as a result of the heat generation. In the table close-ups of the cars are provided which are displayed with a doubling time interval up to 480 seconds after which snap shots are displayed with an interval of 240 [s]. It can be observed that the implementation of the different car fires with three different volumes above the cars where the heat is released separately is successful since the cars start burning within the flashover points as discussed in §4.4.2. Moreover the stratification of the smoke layer due to the density differences is present. The results don't show any irregularities and are considered valid.

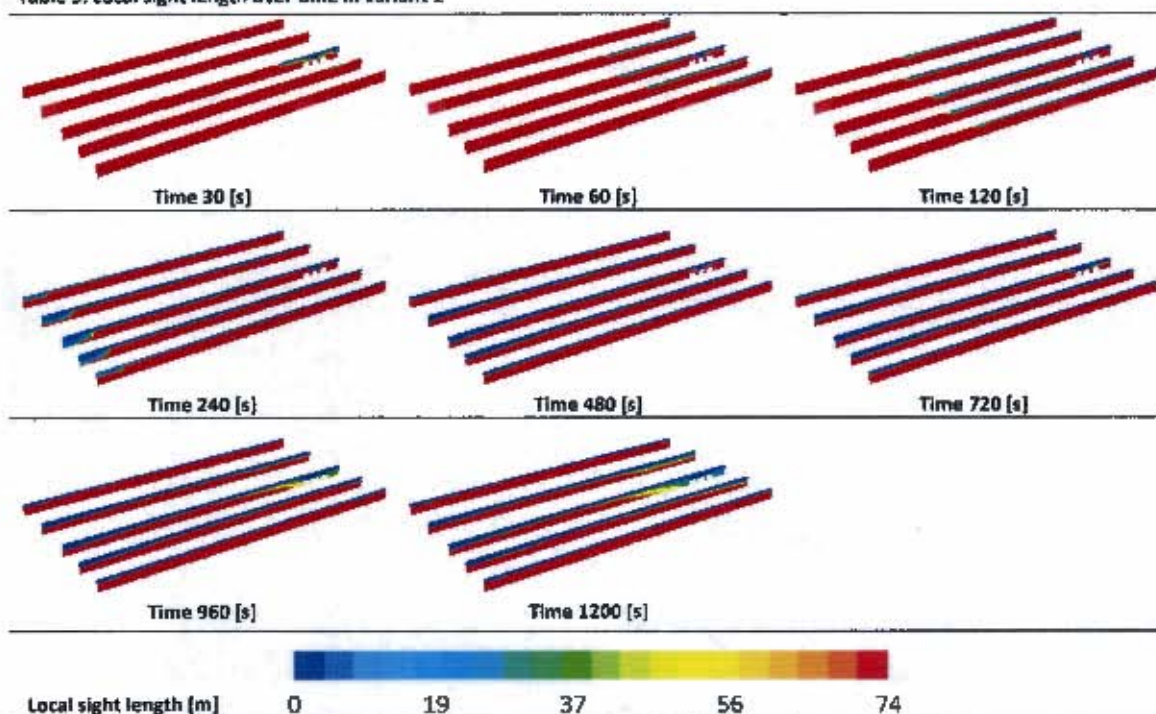
Table 8. Temperature above burning cars in variant 1



The smoke production of the fire in variant 1 is made visible in Table 9 where an isometric view is provided. In the table the local sight length is provided with a minimum of 0 meter and a maximum of 74 meter (this is the longest distance diagonal throughout the car park). Out of the table can be observed how the smoke layer develops throughout the car park, it can be seen that the smoke layer will travel the total length of the car park within 240 seconds (for variant 1). Moreover the expected layering of the smoke layer is visible. These results don't show any irregularities and are considered as valid.










Table 9. Local sight length over time in variant 1.



#### 4.8 Different simulation variants

In order to provide results with the use of CFD which can provide insight in the objective (§3) it is necessary to choose the simulation variants in such a way that they will provide results in both worst case situations and provide insight in the influence of wind induced ventilation in a semi-open car park. The layout of these variants is linked to the outcome of the method discussed in §4.2 and the requirements of the current guidelines. Based on the method and the guideline requirements it is analyzed if statement 1.e.i. or 1.e.ii discussed in §2.4.2 will result in the smallest opening area for the most general dimensions of a semi-open car park. For the proper testing of the guideline some situations will be tested which just meet the requirements stated in the guideline. This will represent the worst case situations. On the other hand to determine the effect of wind induced ventilation on a car fire inside a semi-open car park, an approach is chosen in which the open area of the facade of the car park is maximized to provide a situation in which wind can play a significant role, however this is done with the restriction that it is possible to handle modelling requirements in a accurate way. Sketches of the variants which are analyzed are displayed in Table 10 where the open area is displayed in blue and the cars on fire are coloured red. The used grid for this simulation will be the result of a grid sensitivity study as discussed in §4.5.3. The position of the cars is chosen in such a way that it complies with the general distribution of cars with the geometry of the car park taken into account. In this type of car park it's likely that a road for driving around in the car park is located near the short edges. The cars are therefore placed taking a minimal road width into account (based on NEN2443). For the outside temperature 9.8 [°C] is used, since this the average outside temperature over a year in the Netherlands [51].

Table 10. Description of different simulation variants

	Sketch of simulation variant	Description
Variant 1		In this variant the walls over the length of the car park are completely open. The short sides are closed. Wind effects aren't taken into account. <i>Referred to as: long sides Completely Open No Wind (CONW)</i>
Variant 2		In this variant the openings over the length of the car park are reduced so they match the 33% requirement of the NEN2443 exactly. <i>Referred to as: Long sides Partially Open No Wind (PONW)</i>
Variant 3		In this variant the walls over the length of the car park are completely open. The short sides are closed. A wind pressure is set on the boundary which will result in a wind velocity of roughly 1.5 [m/s]. <i>Referred to as: long sides Completely Open 1.5 [m/s] Wind (CO1.5W)</i>
Variant 4		In this variant the walls over the length of the car park are completely open. The short sides are closed. A wind pressure is set on the boundary which will result in a wind velocity of roughly 5 [m/s]. <i>Referred to as: long sides Completely Open 5 [m/s] Wind (CO5W)</i>
Variant 5		In this variant the openings over the length of the car park are reduced so they match the 33% requirement of the NEN2443 exactly the location is shifted however. <i>Referred to as: Long sides Partially Open and Translated No Wind (POTNW)</i>
Variant 6		In this variant the walls over the length of the car park are open with exception of a 1 [m] high balustrade. The short sides are closed. Wind effects aren't taken into account. <i>Referred to as: Long sides Partially Open and Balustrade No Wind (POBNW)</i>
Variant 7		In this variant the openings over the length of the car park are reduced so they match the 33% requirement of the NEN2443 exactly (statement 1.E.I. in §0). However also structural bearings are taken into account (its dimensions are discussed in appendix 1) <i>Referred to as: Long sides Partially Open and Structural Beams No Wind (POSBNW)</i>

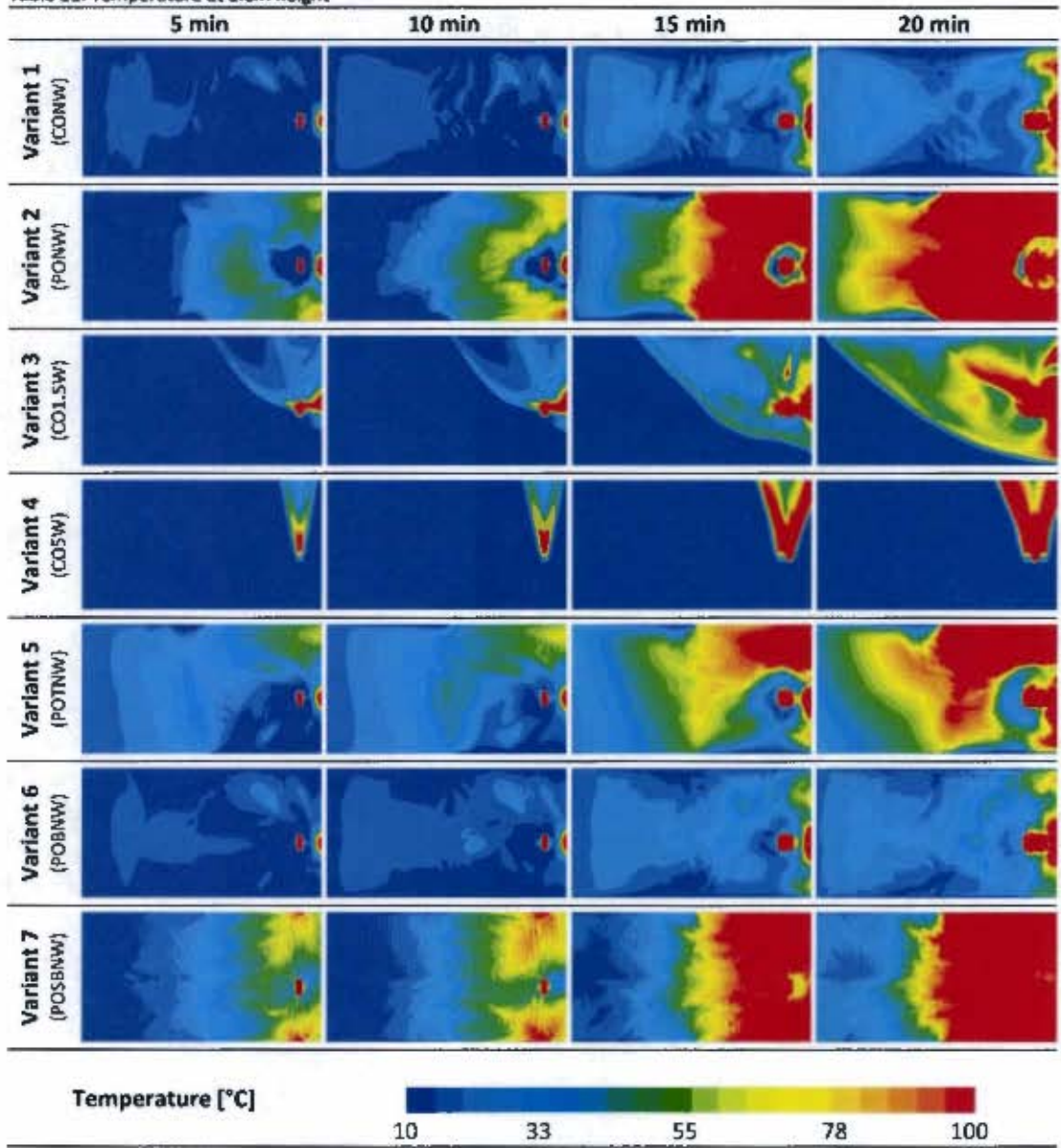
## 5 Results

In this paragraph the results of the different variants are presented. These are separated in the results for the temperature criteria and the sight length criteria.

### 5.1 Temperature safety criteria

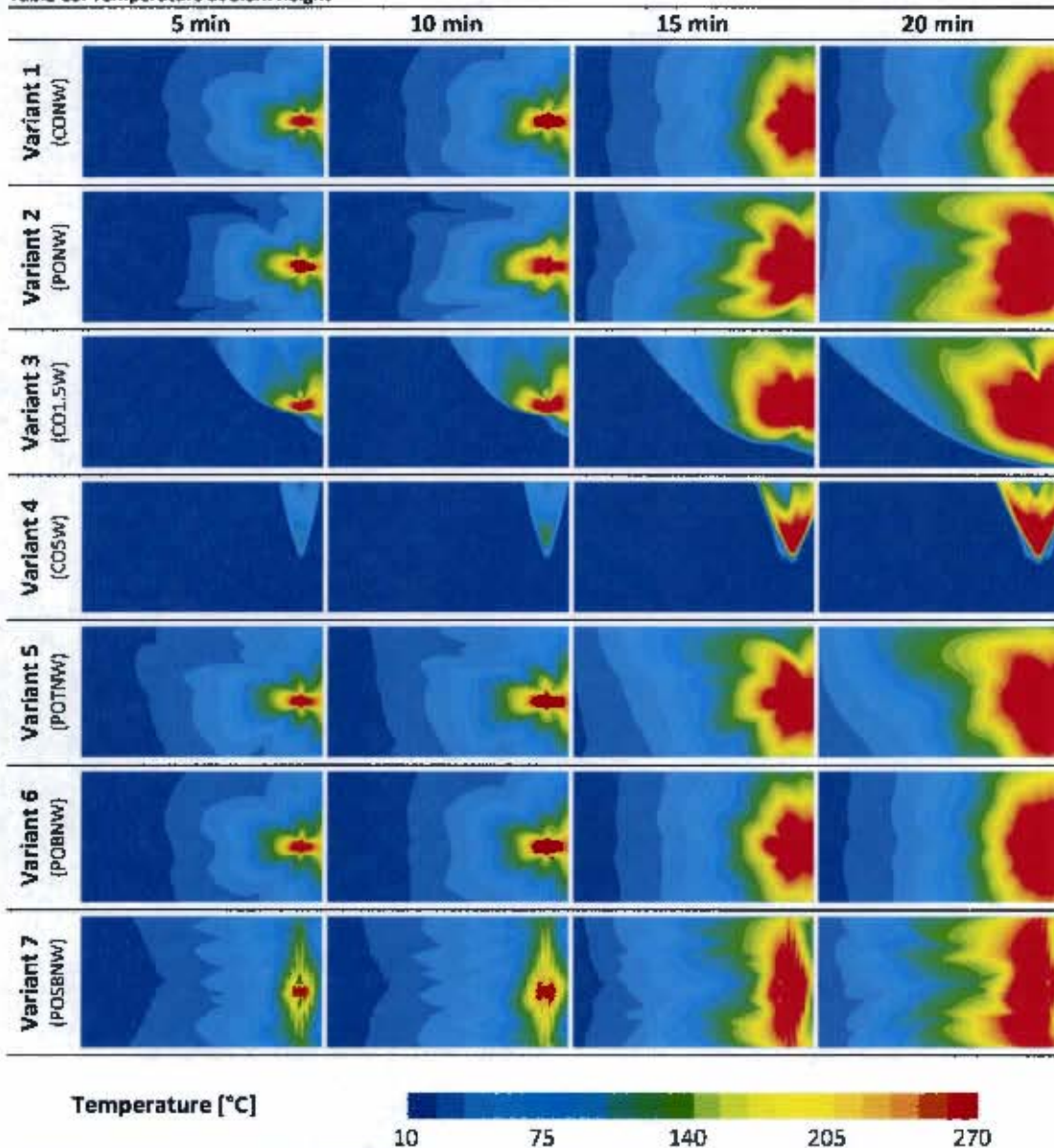
The results considering the safety criteria of the maximum temperatures under which a safe deployment of the fire brigade is still possible (as discussed in §2.2.2) are displayed in Table 11 and Table 12. In these tables the temperatures are displayed at a horizontal plane at 1.8 and 2.3 meter height relatively, with a time interval of 5 minutes. In Table 11 significant differences are visible in the temperature distribution at 1.8 meter height between the different variants. For variants 1, 3, 4 and 6 the magnitude of the area where the temperature is higher than the 100 [°C] criteria is relative small compared to the other variants. Moreover the location of this area is situated near the burning cars, whereas it is largely dispersed for the other variants. When variant 1 and 6 are compared, the results are quite similar, however variant 6 does show temperatures which are slightly higher meaning that the heat removal is affected by the balustrade. When variants 2 and 7 are compared these results are similar on first sight, however the propagation of the high temperatures in longitudinal direction seems to occur with a lower velocity for variant 7 than is the case for variant 1, meaning that the smoke removal is affected by the structural beams. Though both variant 3 as 4 implement wind induced ventilation, a significant difference in behaviour can be observed. It appears that the smoke layer develops into the direction of the wind in variant 3 (back layering of the smoke front). Despite of the wind effects the temperature increases in the longitudinal direction, after 20 minutes this layer has almost travelled the total length of the car park and covered more than 50% of it. This behaviour isn't visible in variant 4 where the area where the temperature increases stays limited to a relative small area, moreover back layering doesn't seem to occur and the propagation in the longitudinal direction is minimal. The results of variant 5 show that the temperature inside the car park will increase over the total length, moreover it appears that the largest increase is found at the closed corner near the burning cars. From this corner the temperature layer expands throughout the car park. At the opposite side of this corner the temperature is significantly lower, meaning that heat is removed by the opening at this location quite effectively.

Table 11. Temperature at 1.8m height



The results of a horizontal plane at 2.3[m] height are displayed in Table 12, notice that the maximum temperature is set to 270 [°C] as discussed in §2.2.2. It can be noticed that the results seem much more identical than was the case at 1.8m height. Variants 1,2,5,6 and 7 show comparable results since the location and magnitude of the area where the temperature is around 270 [°C] seems to be quite similar. Variants 3 and 4 show the largest difference, due to the effect of wind the area with temperatures higher than 270 [°C] changes drastically, however for variant 3 it can be seen that eventually (after back layering is started) the size of the area becomes roughly equal to the other variants. When variant 1 and 6 are compared it is noticed that the surface area of the highest temperature at 20 minutes is just slightly larger for variant 6. Comparing variant 2 and 7 it is shown that the temperature layer is expanded more in perpendicular direction for variant 7 than is the case for variant 2. In variant 5 it's visible that the high temperature layer develops more towards the opening at the bottom edge than in the opposite direction.

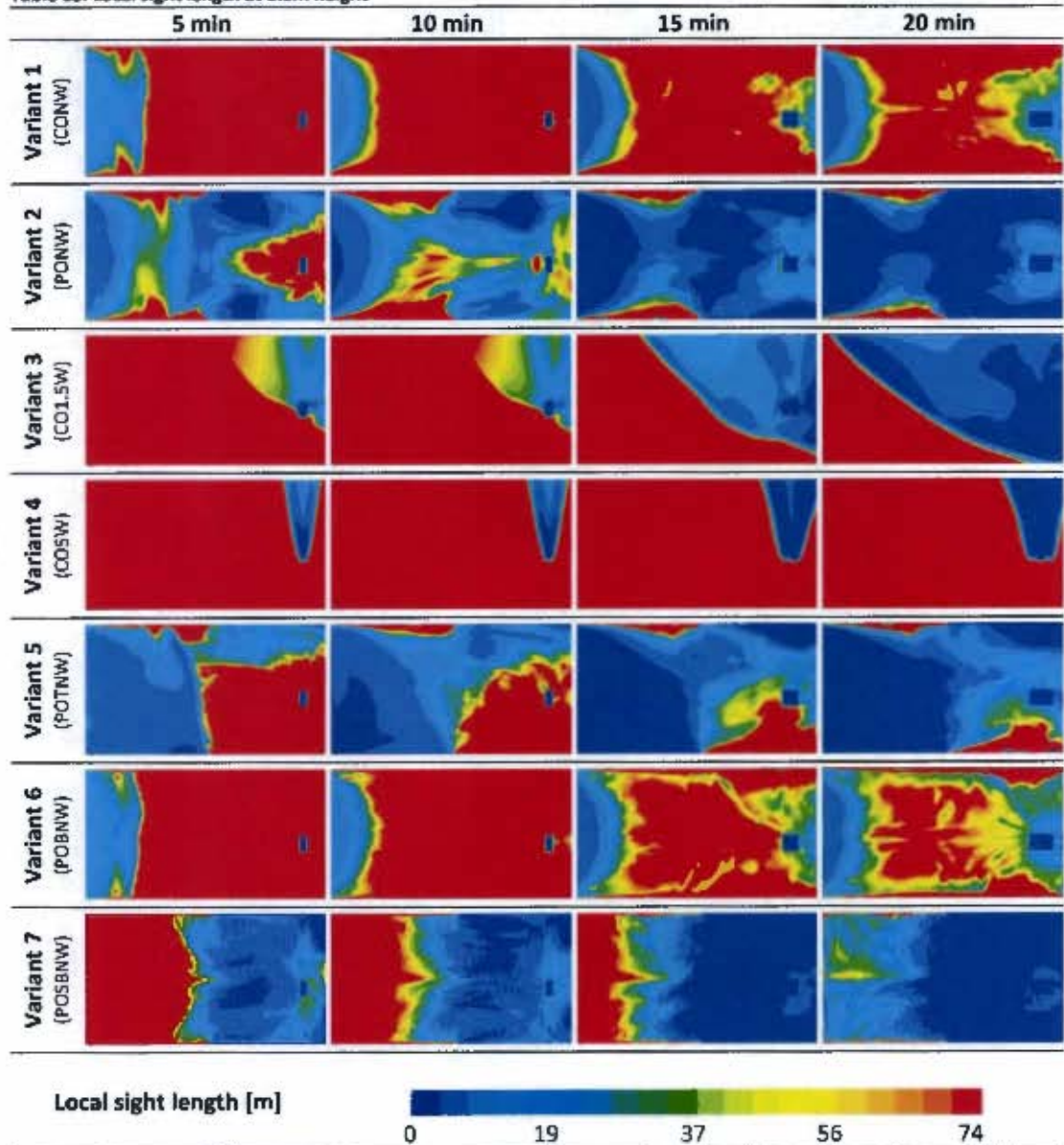
Table 12. Temperature at 2.3m height



## 5.2 Sight length safety criteria

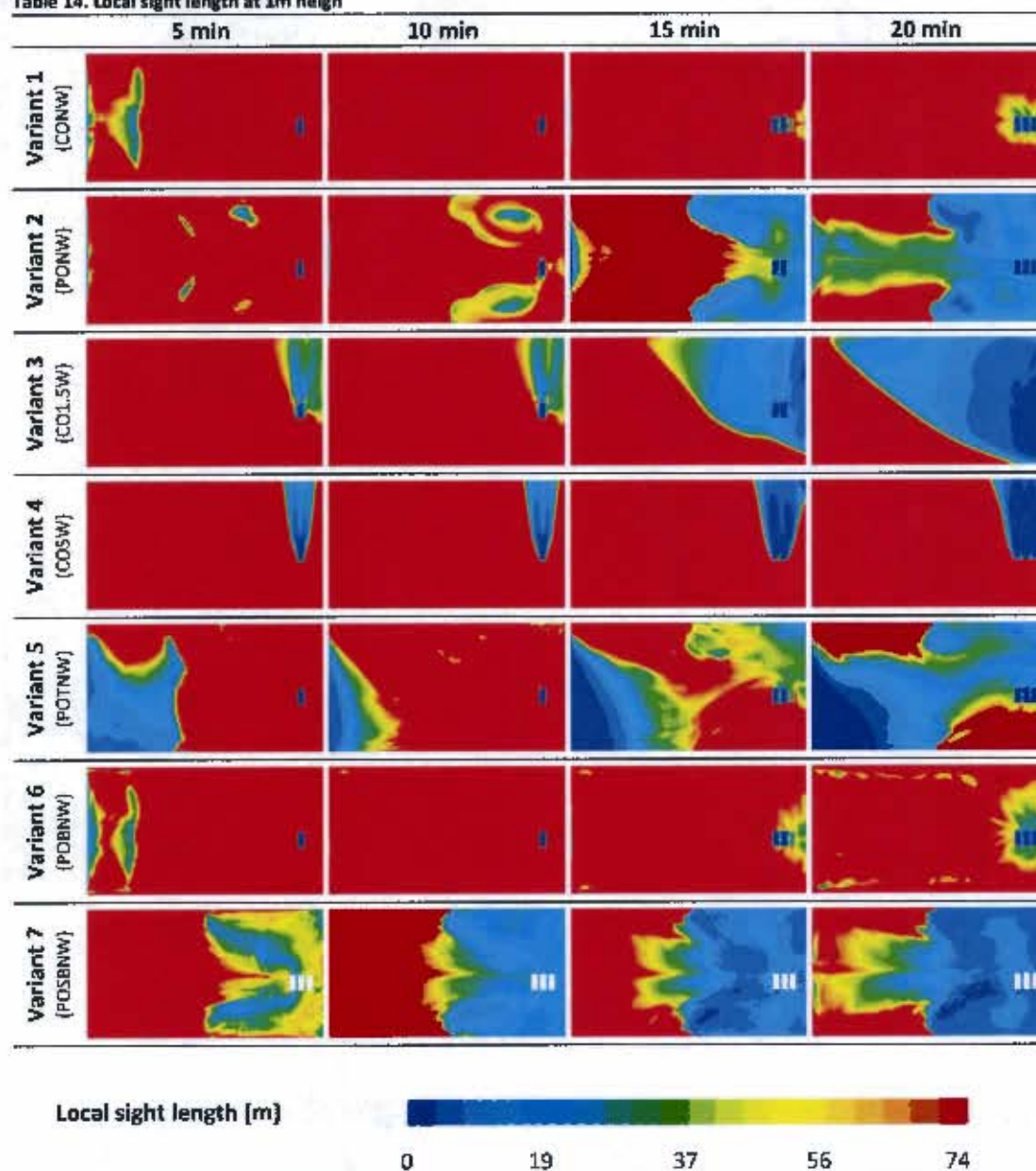
In this chapter the local sight length at different heights will be discussed towards light sources, in Table 13 the local sight length at a horizontal plane at 1.5m is displayed and in Table 14 the local sight length at 1 m height. The results shown in Table 13 provide the sight length dependence on the variant, there exist clear differences between the variants. Observing the results of variant 1, 5 and 6 the smoke layer seems to be created at the opposite side where the car-fire is positioned. This is explained by Table 9 shown in §0. This table shows that the smoke layer travels the length of the car park above 1.5[m] height, and falls below this height at the moments that it meets the opposite wall. This effect also plays a role in variant 2, however due to the presence of the side walls the smoke layer does come down close to the fire as well. Moreover the effect of a smoke layer coming down at the moment it reaches a wall is also visible at the corner near the fire in variant 5.

Table 13. Local sight length at 1.5m height



The smoke layer in variant 7 seems to behave in a different way. Due to the mixing effect caused by the structural beams the smoke layer falls down from the moment it starts developing in the longitudinal direction. The effect of a smoke layer falling down instantly is also visible in variants 3 and 4, where due to the higher turbulence intensity the mixing of the smoke layer is influenced. It can be observed that downstream of the fire the visibility is reduced instantly. For variant 3 this effect is eventually also visible upstream of the wind and in the longitudinal direction as well. In variant 6 the mixing of the smoke layer also plays a role, at 15 and 20 minutes it is visible that near the boundaries over the length of the car park there exist two areas where the smoke layer is lower. This is caused by the higher turbulence created by the effect that in and outflow over the opening are closer together (due to the 1m high balustrade). For variant 5 it appears that the smoke removal throughout the opening nearest to the fire is quite effective. The sight length from the fire towards this opening stays relatively large over the total time span of the fire.

Table 14. Local sight length at 1m height



When the results of Table 14 are taken into account, it is visible that when assessing the visibility the height at which this is done is of importance. The difference between the results at 1.5[m] and 1[m] are significant. The visibility at 1.5[m] is far more limited than the visibility at 1[m] height. At 1 [m] height the burning cars are visible from almost all locations inside the car park for the variants 1, 4 and 6 whereas the visibility after 20 minutes towards the fire is limited for the other variants. An effect that is not visible at 1.5 [m] is the effect of the outside air that is transported towards the fire. For variant 2 it is visible that this new outside air is cooler and therefore lower positioned. This air flow towards the fire creates two large eddies near the closed walls over the length of the car park (after 10 minutes). It eventually appears to create two smoke free areas at 1[m] height whereas the rest of the car park is filled with smoke. This effect is also visible at the opening near the fire in variant 5 where the outside air pushes the smoke layer away, which has a positive effect on the visibility. In variant 7 the effect also occurs near the openings, however the effect is less effective. This is most likely a result of the mixing of the air underneath the structural beams. For the variants 3 and 4 similar results are found as for the case at 1.5 [m] height. At 1[m] height the effect of the higher turbulence intensity is visible as the smoke layer does come down in the downstream direction instantly (in variant 3 eventually also upstream).



## 6 Discussion

In this chapter an analysis will be made on the results of the different variants which are discussed in §4.8 and which results were shown in §5. The analysis will contain a study on the behaviour of the car over the time span of the fire, as well as a direct comparison on certain moments in time. Moreover eventually the area's where a safe deployment of the fire brigade is still possible is provided for each variant.

### 6.1 Analysis of car park behavior over time

In this chapter the CFD-results will be analyzed over the total time span of the car park fire, both an explanation of this analysis approach as the results of this analysis will be provided.

#### 6.1.1 Explanation of analysis approach

The results obtained and shown in §4.7 provided insight in the safety criteria at a 5 minute interval. In order to ensure that these results did provide a good image of the car park behaviour over the total time span of the fire it is desirable to make an analysis which covers this complete time domain at a smaller time interval. This is done by the implementation of a total of 392 monitor points half of which monitoring the temperature at both 2.3 [m] and 1.8 [m] and the other half monitoring the local sight length at 1.5 [m] and 1 [m]. These monitor points are placed on two cross-sections visible in Fig. 44 and Fig. 45.

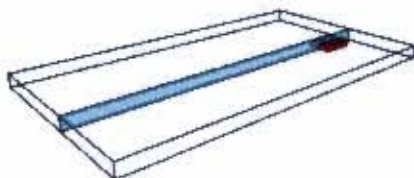


Fig. 44. cross-section in longitudinal direction

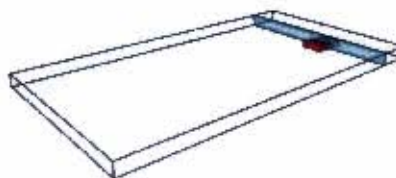


Fig. 45. cross-section in perpendicular direction

The results obtained from these monitor points are plotted in a 3d surface plot, which provides a specific variable as a function of time and location. An example of this is visible in Fig. 46 where the local sight length at 1m height is plotted over time and location for variant 7. As visible in Fig. 47 the results become more clear when they are assessed from a top view. In this graph the location is plotted on the horizontal axes and the time on the vertical axes. It is visible that the first car that is lit is located at 59 [m] since here the local sight length is reduced to zero from the start of the fire. It also is visible how the sight length reduces over the length of the car park with an increase in time. Similar plots are made for the other cross-section and for the other variable (temperature), and will be discussed in the following paragraph.

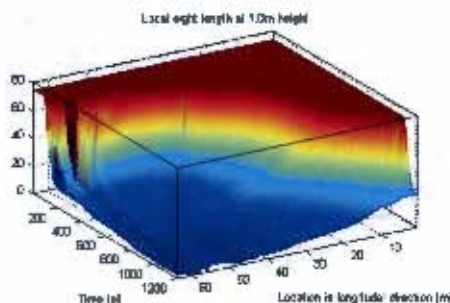


Fig. 46. Surface plot of local sight length at 1m height

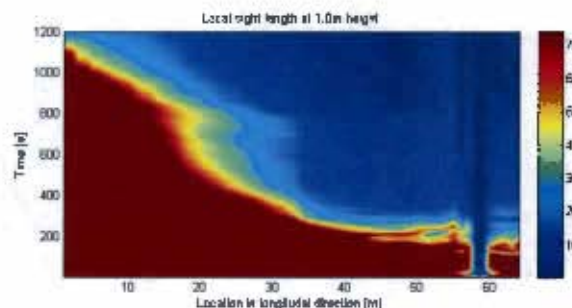


Fig. 47. Top view of local sight length at 1m height

## 6.1.2 Implementation of analysis to different variants

The created surface graphs which are a result of the analysis over the time span of the fire are visible in appendix 4 to 9. It can be seen that for the sight length both the result towards a light source as to a light reflecting object are displayed. The results of both the sight length as the temperature will be discussed. Note that the maximum displayed values are equal to the maximum safety requirements for the temperature (as discussed in §2.2.2) and equal to 74 m for the local sight length (which is the maximum distance in diagonal direction throughout the car park)

### Variant 1 (CONW)

From the results of the local sight length at 1.5[m] height, which is displayed in appendix 8, it can be observed that directly above the fire (at 59[m] in the longitudinal and at 15[m] in the perpendicular direction) the sight length is immediately reduced to zero. However it can also be observed that it is very likely that firemen can see the fire for the entire fire duration and therefore also the necessary 20 minutes after ignition. The area where the sight length is limited is mainly located in a relative small area near the fire. Moreover when the local sight length in perpendicular direction is observed at 20 minutes it can be seen that on the line starting 30 [m] away from the fire towards the fire, the local sight length is larger than 30 [m] for the largest part on this line, which therefore results in an average local sight length which will be larger than 30 [m] over this line. Since this average local sight length is higher than 30 [m] the fire will be visible at 1.5m height and therefore also at 1.0[m] height. Out of the temperatures on head height (1.8 [m]) and on 2.3[m] visible in appendix 4 and 5 can be observed that close to the fire these limits are exceeded however further away from the fire the temperatures are acceptable. The fire brigade can reach the fire from at least one direction to put water on the fire.

### Variant 2 (PONW)

Considering the local sight length at 1.5[m] height as displayed in appendix 8 it can be observed that around 700 seconds after ignition the visibility towards the fire changes dramatically in the longitudinal direction, moreover after 500 seconds the visibility in the perpendicular direction starts to decrease significantly. At 1000 seconds the visibility is reduced to zero meaning that the fire brigade isn't able to see the fire from 30 meter distance any more. This is true for 1.5 [m] height and 1.0 [m] height as well since on the line starting 30 [m] away from the fire towards the fire, the local sight length is lower than this value. Assessing the temperature it can be seen in appendix 4 and 5 that around 600 seconds after the ignition of the car fires the temperature at 1.8 [m] is above the temperature criteria of 100 [°C] constantly. This is visible in both the longitudinal as perpendicular direction. The result of this is that in reality the fire brigade wouldn't be able to approach the fire based upon the temperature criteria for this. Assessing the temperature at 2.3[m] height it's visible that for this height the temperature will exceed the safety criteria close to the fire instantly, however this area increases from around 600 seconds and is increasing from that point forward. This occurs in both the longitudinal as perpendicular direction. Meaning that this safety criteria considering a safe deployment of the fire brigade isn't met either.

### Variant 3 (CO1.5W)

From the local sight length at 1.5[m] height which is displayed in appendix 8 it can be observed that in perpendicular direction in the wake of the fire the visibility reduces to zero in a relative short time interval. The visibility in longitudinal direction starts to decrease at a later point in time, starting from approximately 600 seconds when the second car starts burning. Approximately 100 second later also the visibility upstream the fire in perpendicular direction starts to decrease rapidly. The result is that around 700 seconds after the ignition the fire isn't visible anymore at

1.5[m] height. Due to the high turbulence of the air, the mixing of the smoke layer results in a limited visibility of the fire at 1[m] height as well. Therefore the fire isn't visible for firemen from around 700 seconds. Taking into account the temperatures it can be seen that the temperatures at 1.8 [m] are significantly lower than is the case for variant 2. The temperature criteria at 1.8 [m] height aren't reached meaning that based on these criteria the deployment of the fire brigade would be relatively safe. When the temperature criteria at 2.3 [m] are assessed it is visible that the area at which this criteria is reached increases from the moment that the second car starts burning. Moreover the results aren't equal at both sides of the cars in perpendicular direction. It appears that due to the wind effects the stratification of the smoke layer disappears in such a manner that even the highest temperatures are mixed, resulting in a lower average temperature than is the case when stratification does occur as in variant 1, 2, 5, 6 and 7. Based on these results it is concluded that the criteria at 2.3 [m] height are reached after 600 seconds. However the distance is not more than 10 meter away from the fire.

#### **Variant 4 (COSW)**

Considering the local sight length at 1.5[m] height as displayed in appendix 8 it can be observed that in perpendicular direction in the wake of the fire the visibility reduces to zero in an even more rapid manner than was the case for variant 3. However from the visibility doesn't change upstream the fire or in the longitudinal direction. Therefore the requirements based upon the safety criteria regarding the sight length are met. Observing the temperatures it is concluded that the wind has a significant influence on this variable. During the time span of the fire it can be approached by the fire brigade in a relatively safe manner in both the longitudinal and upstream in perpendicular direction.

#### **Variant 5 (POTNW)**

The local sight length at 1.5[m] height, displayed in appendix 8 it shows that at 1.5 [m] height the visibility changes gradually in longitudinal direction. After 20 minutes the visibility is minimal. However when a line starting 30 [m] away from the fire towards the fire is considered, it is visible that after 20 minutes the local sight length over this line is never lower than the distance towards the fire. Therefore it's concluded that the fire is visible at 1.5 [m] height in perpendicular direction for the total time span of the fire. This is also true for the other direction and height. Therefore it is concluded that based upon the sight length the fire brigade can reach the fire in a relatively safe manner. With respect to the temperatures it is shown that at 1.8 [m] height the temperature criteria will be reached if the distance up to the fire is more than 10 meters. This is valid both in the longitudinal as the perpendicular direction around 900 seconds after ignition. However there also exists an area where the temperature criteria is not met. Considering the temperature criteria at 2.3 [m] this criteria is not met in perpendicular direction within 20 minutes. Based upon the temperature criteria it can therefore be stated that there are rather large areas where safe deployment of the fire brigade isn't possible, nevertheless it's possible for firemen to reach the area between the areas where the criteria are not met. From those positions it is possible to extinguish the fire.

#### **Variant 6 (POBNW)**

Considering the local sight length at 1.5[m] height as displayed in appendix 8 at 1.5 [m] height visibility is comparable to the visibility as discussed for variant 7. The visibility criteria are met at 1.5[m] and 1 [m]. Therefore the fire brigade can reach the fire in a relatively safe manner. When assessing the temperature criteria it's visible that these are (as well as discussed for variant 1) met at a 1.8[m] height for both directions. In addition it can be observed that the criteria for 2.3 [m] height are met in the longitudinal direction whereas in the perpendicular direction these conditions aren't met, allowing one direction for the firemen to approach the fire.

#### **Variant 7 (POSBNW)**

The local sight length at 1.5[m] height presented in appendix 8 show that at 1.5 [m] height visibility does change most rapid of all simulated variants. The smoke layer reaches this height about 100 seconds after ignition in longitudinal direction. The smoke layer expands constantly from this point forward. In perpendicular direction the visibility changes in an equally rapid manner. At 1[m] height the smoke layer does change rapidly after 100 seconds as well. The visibility toward the fire is reduced to zero after about 800 seconds. For the fire brigade this will result in zero visibility which makes a safe deployment impossible. Considering the temperature criteria it's visible that at 1.8 [m] height the temperature starts to increase constantly about 600 seconds after ignition. The distance from the edge of this layer is more than 10 meters from the fire within the time span of the simulated fire. This is true in both the perpendicular as the longitudinal direction. Based on this criterion a safe deployment of the fire brigade therefore isn't possible. Moreover assessing the temperature at 2.3 [m] it's visible that the safety criteria considering this height are not met in perpendicular direction within approximately 900 seconds after ignition.

## 6.2

### Analysis on bases of direct comparison on specific location

In order to provide a better relation between variants a direct comparison on a specific location in the car park is made. This comparison is based both on the temperature and the sight length criteria. In Fig. 48 the graph is visible in which the temperatures on 1.8[m] height and 10 meters remote from the first car are displayed. In this graph the time is displayed on the horizontal axis and the temperature on the vertical one. It is visible that variant 2, 7 will reach the maximum value of 100 [°C] within 20 minutes. The relation between the different variants can be assessed. When the temperature on 1.8[m] height is taken into account, the order in which the different variants can be placed based on their performance from best to worst is variant: 4, 1, 6, 5, 3, 7, 2. A similar assessment can be made at 2.3[m] height. This is displayed in Fig. 49 which shows that the maximum temperature is reached at 2.3[m] height in variant 2 and 3. A clear distinction in performance from best to worst is hard to make since differences in results are relatively small.

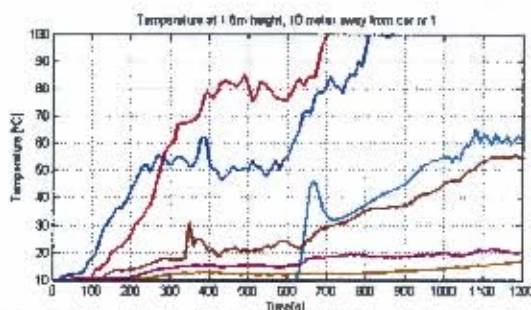
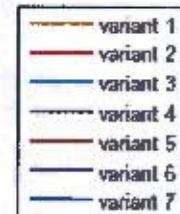


Fig. 48. Temperature at 1.8 meter height over the time span of the fire, 10 meter away from car nr 2

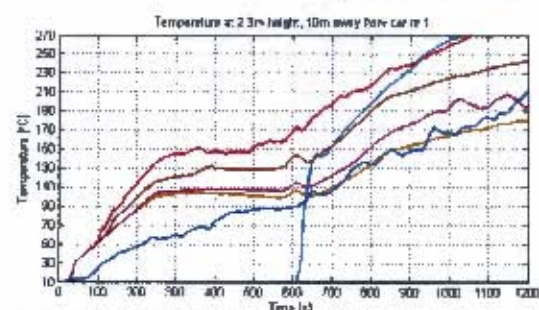


Fig. 49. Temperature at 2.3 meter height over the time span of the fire, 10 meter away from car nr 1

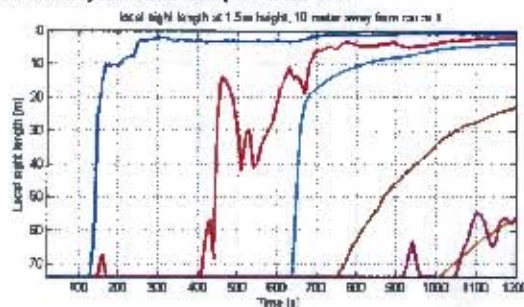


Fig. 50. Local sight length at 1.5 meter height over the time span of the fire, 10 meter away from car nr 1

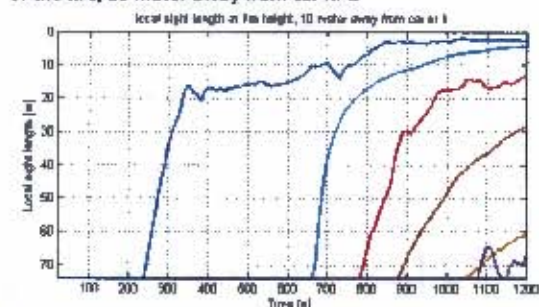






Fig. 51. Local sight length at 1 meter height over the time span of the fire, 10 meter away from car nr 1

It can be observed that variant 2,3 and 5 perform worse than variant 1, 6 and 7 on this safety criteria. The results for the sight length are shown in Fig. 50, where on the horizontal axes the time, and on the vertical axes the local sight length is displayed. For variant 2, 3 and 7 a rapid decrease in visibility is shown. From best to worst the variants can be placed in the following order: 4, 6 & 1, 5, 3, 2, 7. Variant 1 and 6 perform at a similar level based on this sight length criteria. Eventually the safety criteria regarding the sight length at 1[m] height is assessed (Fig. 51). The results are comparable to the 1.5[m] height, however at 1[m] height variant 2 shows a better performance than variant 3.

### 6.3

## Area of car park which is approachable for the fire brigade

As an extension of the analysis, in this paragraph the obtained results for each variant from the temperature and sight length criteria are combined into one figure. This is shown in Fig. 52 to Fig. 58 where different hatched areas are presented. These areas represent unsafe areas for firemen to approach the fire with an interval of 5 minutes starting 10 minutes after ignition of the fire. These areas are based upon the 1.8[m] height temperature, the temperature at 2.3[m] height and the visibility toward light source at 1.5[m] height. An explanation on how these figures are created is provided in appendix 3. The legend of these figures is displayed below:

	= Safe area for firemen	@ time $\leq$ 20 minutes
	= Unsafe area for firemen	@ time $\geq$ 10 minutes
	= Unsafe area for firemen	@ time $\geq$ 15 minutes
	= Unsafe area for firemen	@ time $\geq$ 20 minutes

The white areas will be relatively safe for firemen to approach the fire over the total time span of the fire. The hatched area will be unapproachable after a certain time interval because the temperature will be too high or visibility towards the fire is too low. This analysis shows that there are significant differences between the seven variants. It varies from almost an entire car park area which is approachable, to an inapproachable area that covers the complete car park after 10 minutes. Furthermore for variants 1, 4 and 6 the unapproachable area is limited to the location close to the fire. Based on these results it can therefore be stated that in a fire situation the firemen will be able to approach the fire relatively safe and extinguish it. For the variants 2, 3 and 7 there isn't an area available which allows an approach in a safe manner after 20 minutes. For variant 2 and 7 this is the case after 15 minutes whereas for variant 3 this is the case after 20 minutes. Variant 3 therefore is significantly safer than variant 2 and 7 through they all do not meet the safety criteria. Comparing variant 2 and 7 it's visible that in variant 7 the inapproachable area after 10 minutes is larger than for variant 2, meaning that the performance of variant 7 is more worse than variant 2. Variant 5 indicates that there exists an area which is approachable for firemen, however this area is surrounded by area's in which the temperature will exceed the safety criteria. It's therefore questionable if it's really safe for firemen to enter this area, because it's possible that in the situation that the firemen aren't capable/able to extinguish



Fig. 52. Variant 1 (CONW), unsafe area

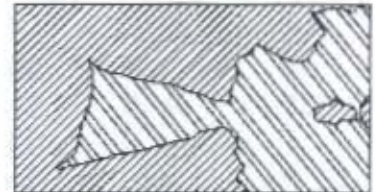


Fig. 53. Variant 2 (PONW), unsafe area

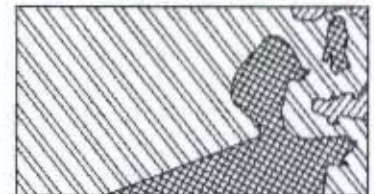


Fig. 54. Variant 3 (CO1.5W), unsafe area



Fig. 55. Variant 4 (COSW), unsafe area



Fig. 56. Variant 5 (POTNW), unsafe area



Fig. 57. Variant 6 (POBNW), unsafe area



Fig. 58. Variant 7 (POS8NW), unsafe area

the fire within 20 minutes they can be trapped inside this area. Based on the 20 minutes criteria variant 5 is considered as relatively safe with the remark that it's safety level is significantly lower than is the case for variant 1, 4 and 6.

## 6.4 Safety level assessment for all variants

Based upon the analysis provided in the previous chapters, it's possible to provide a final assessment on the safety level of each variant, in Table 15 this assessment is provided. Each criteria is assessed in two directions namely the longitudinal direction (x dir) and the perpendicular direction (y dir). In the case that a safety criteria is reached within 20 minutes it's time will be displayed in red. This time is displayed in minutes. When the criteria are not met in two different directions this will result in an insufficient safety level, because there isn't approachable direction towards the fire.

Table 15. Safety level assessment for all variants with on bases of safety criteria.

variant	Sight length				Temperature				Safety level assessment
	1 [m]		1.5 [m]		1.8 [m]		2.3 [m]		
	x dir	y dir	x dir	y dir	x dir	y dir	x dir	y dir	
1	20	20	20	20	20	20	20	<20	sufficient
2	≤20	20	≤15	≤15	≤15	≤10	≤15	<20	insufficient
3	≤15	≤15	≤15	≤15	20	20	<20	20	insufficient
4	20	20	20	20	20	20	20	20	sufficient
5	20	20	20	20	20	<20	20	<20	questionable
6	20	20	20	20	20	20	20	<20	sufficient
7	≤15	≤15	≤5	≤10	≤15	≤10	20	≤15	insufficient

<sup>\*)</sup> There is an area which complies with the safety criteria, however this area is surrounded by area which don't comply. Its safety is therefore questionable.

The assessment of the safety level is provided in the most right column of Table 15. This shows a sufficient safety level for variant 1, 4 and 6 and an insufficient safety level for variants 2, 3 and 7. Moreover it visible that the safety level of variant 5 is assessed to be questionable, this is a result of the temperature criteria at 1.8[m] height in longitudinal direction.

Based upon the seven different variants which are assessed, the sub questions can be answered:

- *What are the general car park dimensions in the Netherlands?*  
Based on an assessment of 65 car parks in the Netherlands it can be concluded that the most general car park dimensions are between 55 and 65 meter in length and between 20 to 35 meter in width.
- *Does the influence of wind provide a higher safety level in all cases when compared to a situation without wind?*  
The presence of wind doesn't provide a higher safety level in all cases when compared to the same situation without wind. However it can also be concluded that when wind pressures are present which lead to air velocities inside the car park around  $5 \text{ [m}^1\text{s}^{-1}]$  this will ensure safe upstream situations.
- *Does the distribution and location of the opening area in the façade of the car park have a significant influence on the fire safety level?*  
If the open façades are mainly placed on one end in comparison to a distribution over the complete length, will the fire safety level significantly.
- *Have structural beams placed at ceiling height a significant influence on the fire safety level?*  
Structural beams placed perpendicular on the mean smoke layer direction will result in a higher mixing of this smoke layer with the fresh air underneath, which reduces the visibility towards the fire and safety level significantly.
- *Does the presence of a balustrade affect the fire safety level significantly compared to a situation without a balustrade?*  
Taking into account a balustrade of 1 meter height it appears that this doesn't have a significant influence on the safety level as long as the façade in longitudinal direction are completely open for the remaining area.

Based upon the findings in the research, the research question can be answered:

*To what extent is there a risk in the safe deployment of the firebrigade during a car fire in a semi-open car park, when the amount of natural ventilation is in line with the conditions as stated in current Dutch guidelines, and when wind-effects as well as potentially worst-case scenarios are taken into account*

There potentially exist a significant risk in the safe deployment the the firebrigade during a car fire in a semi-open car park when the amount of natural ventilation is in line with the conditions as stated in current Dutch guidelines. Moreover wind effects should be considered in the design since it influences the safety level significantly.



## 8 Recommendations

As a result of the research described in this report new research questions did arise. Following recommendations for future research are made.

### Car park properties related:

- To perform an assessment with other types of car parks as well.
- To perform a CFD-simulation in which the car park is filled with cars, in order to assess the influence of not taken this into account.
- Internal ramps aren't taken into account in the simulation, for further research the influence of these ramps could be determined.
- The openings used in the simulation were all completely open, in reality it is known that perforated plates or plants are placed at these openings. The influence that this has on the safety level is still unknown and open for future research.
- To determine how many car-parks in the Netherlands are comparable to variant 2, 5 and 7 in order to determine the fire safety level of current car parks.

### Fire research related:

- The smoke production of cars is based on relatively old research in which old cars were set on fire. New cars contain more plastics which would potentially lead to a higher smoke production. Therefore research on the smoke production of new cars would lead to a higher accuracy of the simulation results.
- In this research it's assumed that when the temperature is too high more than 10 meters from the fire, the fire can't be extinguished by the fire brigade. An investigation on this distance should show if this is a correct assumption.

### Modelling related:

- To perform CFD-simulations with different fire curves in order to assess the influence of the fire curve has on the results.
- It has become clear that when the air velocity (created by wind) changes from 1.5 [ $\text{m}^1\text{s}^{-1}$ ] to 5 [ $\text{m}^1\text{s}^{-1}$ ] the fire safety level increases significantly. The air velocity at which a sufficient safety level is obtained can now be determined.
- It has become clear that a balustrade of 1 meter does not result in a significant lower safety level. The height at which this does result in a strong decrease in the safety level can be determined.
- It has become clear that 1/3 open area criteria can lead to an insufficient safety level. The minimum open area where the safety level changes from sufficient to insufficient can now be determined.

- [1] Centaal Bureau voor de Statistiek (2010) Motorvoertuigen; aantal voertuigen en autodichtheid per provincie, URL: <http://statline.cbs.nl/StatWeb/>
- [2] G.A.P. Brouwer (2009) Effectiviteit van verticale ventilatieopeningen in een zone model, BSc thesis, Christelijke Hogeschool Windesheim, School of Built environment & Transport, Zwolle
- [3] M. Ahrens (2004) U.S. vehicle fire trends and patterns. Fire Analysis and Research Division National Fire Protection Association 1-12
- [4] P. Wijnhoven, I.M.M.M.C Naus, W. Zeiler (2008) Invloedsfactoren en risico's bij brand in parkeergarages 3-9
- [5] D. Joyeux, J. Kruppa, L. Cajot, J. Schleich, P. Leur, L. Twilt (2001) Demonstration of real fire tests in car parks and high buildings 53-66
- [6] Y. Li, M. Spearpoint (2004) Assessment of Vehicle Fires In New Zealand Parking Buildings 48-99
- [7] M. Shipp (2009) Fire Spread in Car Parks, CEN TC191 SC1 WG9 SECO Brussels 8-18
- [8] G. Ramachandran (1988) Probabilistic Approach To Fire Risk Evaluation, Fire Technology 24 204-226
- [9] A. Vrouwenvelder (1993) Actions on Structures: Fire, International Council for Building Research Studies and Documentation, the Netherlands
- [10] D. J. Rasbash, D. Ramachandran, B. Kandola, J. M. Watts, M. Law (2004) Evaluation of Fire Safety. John Wiley & Sons, Ltd.
- [11] A. P. Chrest, M. S. Smith, S. Bhuyan, M. Iqbal, D. R. Monahan (2000) Parking Structures: Planning, Design, Construction, Maintenance, and Repair 3<sup>rd</sup> edition. Chapman & Hall, New York.
- [12] Wikimedia Foundation, inc. (2010) Christchurch, URL: <http://nl.wikipedia.org/wiki/Christchurch>
- [13] Wikimedia Foundation, inc. (2010) Amsterdam, URL: <http://nl.wikipedia.org/wiki/Amsterdam>
- [14] S.T.G.D. Hegeman, J. Hensen, M.G.L.C. Loomans, A.D. Lemaire, L.M. Noordijk (2008) Smoke movement in fire situations, CFD-utilization in car park Fleerde. Eindhoven University of Technology.
- [15] TNO Bouw (1997) report 1997-CVB-R0883
- [16] PRC Bouwcentrum (1997) Vluchten bij brand uit grote compartimenten. Bepalingsmethode voor veilig vluchten.
- [17] Bouwdienst Rijkswaterstaat Steunpunt tunnelveiligheid (2002) Safety Proef, rapportage Brandproeven, Utrecht

- [18] H. Ingason (2008) UPTUN, Workpackage 2 Fire development and mitigation measures D221, Target criteria, official UPTUN deliverable version september 2008.
- [19] M.M.M.C. Naus, A.D. Lemaire, V.J.A. Meeussen (2009) Eerste voorstel toetskader bestaande open en gesloten parkeergarages, Efectis report, Rijswijk
- [20] NEN6098 (2010) 2<sup>e</sup> Ontwerp norm, Rookbeheersingssystemen voor mechanisch geventileerde parkeergarages: ICS 13.220.20; 91.140.99
- [21] J. Hill (2005) Car park designers' handbook, Thomas Telford, London
- [22] A. de Jong (2003) Bouwbesluit 2003.
- [23] Staatsblad 410 van het Koninkrijk der Nederlanden (2002) Voorschriften omtrent het bouwen waarvoor het vereiste van een bouwvergunning niet geldt, en omtrent het bouwen waarvoor een lichte bouwvergunning vereist is.
- [24] Oranjewoud SAVE, EFPC, VZBO advies (2007) Beheersbaarheid van brand, Intergrale leidraad
- [25] NEN2443 (2000) parkeren en stallen van personenauto's op terreinen en garages, ICS 91.040.99
- [26] NEN1087 (2001) Ventilatie van gebouwen – bepalingmethoden voor nieuwbouw, ICS 91.140.30
- [27] W.H. Knoll, E.J. Wagenaar (1994) handboek Installatietechniek, ISSO, TVVL, NOVEM
- [28] Landelijk netwerk brandpreventie (2002) praktijkrichtlijn brandveiligheidseisen op het bouwbesluit voor mechanisch geventileerde parkeergarages met een gebruiksoppervlakte groter dan 1000m<sup>2</sup>
- [29] Regionale commissie bouwen en infrastructuur (2008) Praktijkrichtlijn brandveiligheid parkeergarages
- [30] Hobone B.V. (2006) Brandveiligheid stalen parkeergarages, Hoesch additiv Decke, Veenendaal
- [31] A.C. Burns, R.F. Bush (2006) principes van marktonderzoek, toepassingen met SPSS, ISBN-10 9043011304
- [32] B.J.E. Blocken, M.G.L.C. Loomans (2007) introduction to CFD in building engineering, college sheets, Eindhoven University of Technology
- [33] Fluent Inc. (2006). Fluent 6.3 User's Guide. Fluent Inc., Lebanon
- [34] Rehva Guidebook (2007) Computational Fluid Dynamics in ventilation Design
- [35] CFD-online (2010) URL: [http://www.cfd-online.com/Wiki/Law\\_of\\_the\\_wall](http://www.cfd-online.com/Wiki/Law_of_the_wall)
- [36] J. Wieringa (1992) Updating the Davenport roughness classification, Journal of Wind Engineering and Industrial Aerodynamics 41 357-368.
- [37] T. Stathopoulos, R. Storms (1986) Wind environmental conditions in passages between Buildings, Journal of Wind Engineering and Industrial Aerodynamics 24 19-31.

- [38] P.J. Richards, R.P. Hoxey (1993) Appropriate boundary conditions for computational wind engineering models using the  $k-\varepsilon$  turbulence model, *Journal of Wind Engineering and Industrial Aerodynamics* 46 145-153.
- [39] W.D. Janssen, T. van Hooff, B.J.E. Blocken (2010) CFD simulation of wind conditions at the campus of Eindhoven University of Technology, *Eindhoven University of Technology*
- [40] T. van Hooff, B.J.E. Blocken (2010) Coupled urban wind flow and indoor natural ventilation modeling on a high-resolution grid: A case study for the Amsterdam ArenA stadium, *Environmental Modeling & Software* 25 51-65
- [41] ASHRAE Handbook, Fundamentals (SI) (2009) Wind pressure on buildings 24-26
- [42] L.H. Hu, R. Huo, Y.Z. Li, H.B. Wang, W.K. Chow (2004) Full-scale burning tests on studying smoke temperature and velocity along a corridor. *Tunneling and Underground Space Technology* 20 223-229.
- [43] V.I. Blinov, G.N. Khudiakov (1961) Diffusion Burning of Liquids, U.S. Army Translation, NTIS No. AD296762.
- [44] NEN6098 (2010) 2<sup>e</sup> Ontwerp norm, Rookbeheersingssystemen voor mechanisch geventileerde parkeergarages: ICS 13.220.20; 91.140.99
- [45] N.J. Oerle, A.D. Lemaire, P.H.E. van de Leur, (1999) Efficiency of thrust ventilation in closed car parks, Fire tests and simulations. TNO Report 1999-CVB-RR1442
- [46] A.D. Lemaire, R.J.M. van Mierlo, (2009) Rook en rookproductie tijdens brand, Efectis Report, Rijswijk
- [47] G.H. Yeoh, K.K. Yuen (2009) Fluid Dynamics in Fire Engineering, Theory Modelling and Practice, ISBN 9780750685894
- [48] M.A. Sultan (1996) A model for predicting heat transfer through non-insulated unloaded steel-stud gypsum board wall assemblies exposed to fire, *Fire Technology* 32, 3
- [49] European Committee for Standardization (2001) Design of concrete structures - Part 1.2 General rules - Structural fire design, Eurocode 2, Brussels
- [50] P. J. Dinunno, D. Drysdale, C.L. Beyler, W.D. Walton, R.L.P. Custer, J.R. Hall, J.M. Watts (2002) SFPE Handbook of Fire Protection Engineering
- [51] Koninklijk Nederlands Meteorologisch Instituut (2010) het nationale data- en kenniscentrum voor weer, klimaat en seismologie, URL: [http://www.knmi.nl/kd/normalen1971-2000/gemiddelde\\_jaartemperatuur.html](http://www.knmi.nl/kd/normalen1971-2000/gemiddelde_jaartemperatuur.html)

# 10 Appendixes

## Appendix 1, determination of dimensions of structural bearings

In this section the dimensions of the structural bearings of simulation variant 7 are discussed. The dimensions of the double T elements are based on a  $2 \text{ [kN}^2\text{m}^{-2}\text{]}$  load which complies with the calculations in NEN6702 for structural bearings. The geometry and dimensions of the used elements are visible in Fig. 59 and the graph out of which the dimensions are determined is visible in Fig. 60. Moreover the implementation into CFD can be seen in Fig. 61 and Fig. 62.

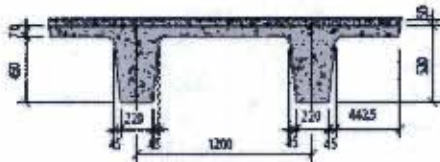


Fig. 59. used dimensions for CFD simulation

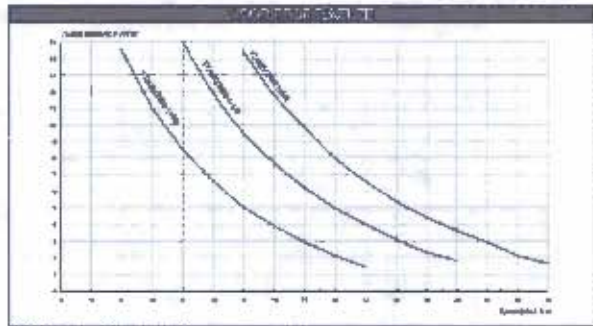


Fig. 60. Graph out of which the dimensions of the double T element are determined

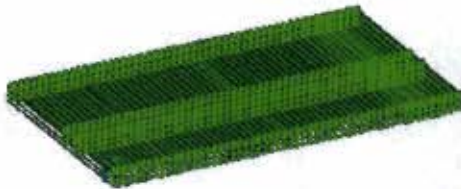


Fig. 61. Overview of total model in gambit

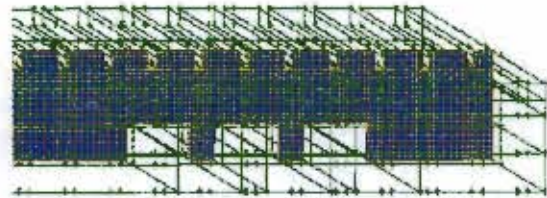


Fig. 62. Detail of grid in area around the cars

## Appendix 2, study on general car park dimensions

In the figure below the pinpointed bird eye images of the car parks taken into account for the identification of general car park dimensions can be seen. Addresses are displayed underneath the picture. The addresses and place (all in the Netherlands) are displayed for the car parks from left to right from the first row to the next.



Fig. 63. Pinpointed bird eye images by the use of satellite maps

Mathildelaan 2 Eindhoven| Korte Kolfstraat 235 Dordrecht| Henri Dunantstraat 5 Heerlen| Kaardesteeg 11 Leiden| Zwaanstraat Tilburg| High-tech campus Eindhoven| Handelsplein 51 Amstelveen| Stadsplein 101 Amstelveen| Handelsplein 51 Amstelveen| Bijlmerplein 700 Amsterdam| Beursplein 15 Amsterdam| Van Bleiswijkstraat 8 Amsterdam| Albert Schweitzerlaan 131 Apeldoorn| Laan 5 - 7 Den Haag| Lutherse Burgwal 25 Den Haag| Lutherse Burgwal Den Haag| Amsterdamse Veerkade 30 Den Haag| Schimmelt 50 Eindhoven| Michelangolaan Eindhoven| Ekkersrijt Eindhoven| Van Loenshof 62 Enschede| Lem Dulstraat 3 Gouda| Stationstraat 28 Heerlen| Klompstraat 11 Heerlen| Putgraaf 10 Heerlen| Uilestraat 4 Heerlen| Schapenkamp 12 Hilversum| Draverslaan 11 Hoofddorp| Prof. Debeyelaan 31 Maastricht| Aert van Nesstraat 16 Rotterdam| Weena zuid Rotterdam| Kromme elleboog Rotterdam| G. J. de jonghweg Rotterdam| Geerweg 4 Sittard| Sint Jacobsstraat 1 Utrecht| Paardenveld 9 Utrecht| Rijnkade 16 Utrecht| Croeselaan Utrecht| Strosteege 43 Utrecht| Leeuwenstraat 2 Rotterdam| Crispijnstraat 8 Rotterdam| Jaarbeursplein 26 Utrecht| Griffioenlaan 1 Utrecht| Pelsterstraat 15 Groningen| Popkenstraat 5 Groningen| Nieuwe parklaan Den Haag| Pijkestraat 1Nijmegen| Spoorhaag Houten| Prinsessesingel Venlo| Arsenaalplein Venlo| Veemarktstraat Tilburg| Korte Breehof Dordrecht| Van Godewijckstraat Dordrecht| Houtkopersplaats Dordrecht| Ir. J.P. van Muijlwijkstraat 175 Arnhem| Erasmusdomein 14 Maastricht| Torenlaan 18 Assen| Mercuriusplein 211 Assen| Floridaplein 2 Haarlem| De Witstraat 2a Haarlem| Regisseurstraat 5 Almere| Regisseurstraat 1 Almere| Schoutstraat 110 Almere| Muntmeesterhof 82 Almere| Concordiastraat 13 Breda| Stationsplein 6 Enschede| Albinusdreef 2 Leiden| Langegracht 3 Leiden| Stationsplein 1 Zwolle| Assiesstraat 2 Zwolle| Van Wevelinkhovenstraat 8 Zwolle| Westerstraat 250 Emmen| Op de Keizer 1 Deventer| Wilhelminalaan 12 Alkmaar| Dijk 16 Alkmaar|

### Appendix 3, determination of area for visibility towards fire

In this section can be seen how the border intill where there is visibility towards the fire is defined out of the local sight length. Its visible that this is based on an estimation of the sight length in a certain direction. This estimation is drawn on the contours by the use of half circles, the border is drawn on the edges of these circles.

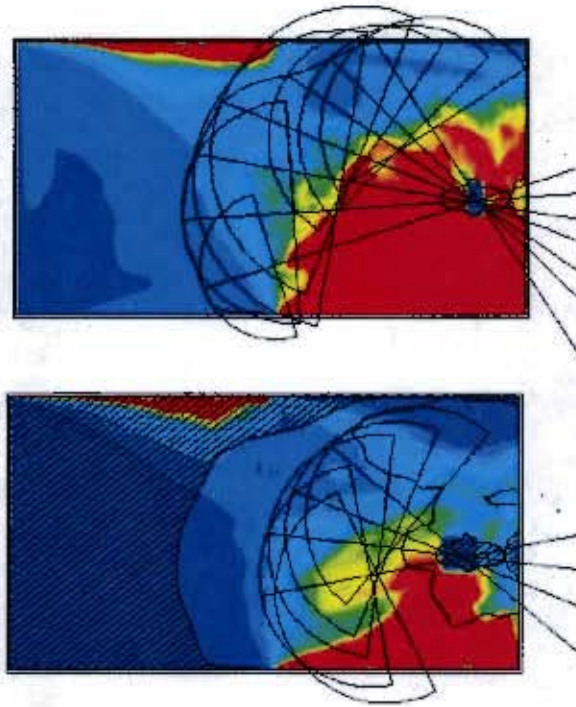
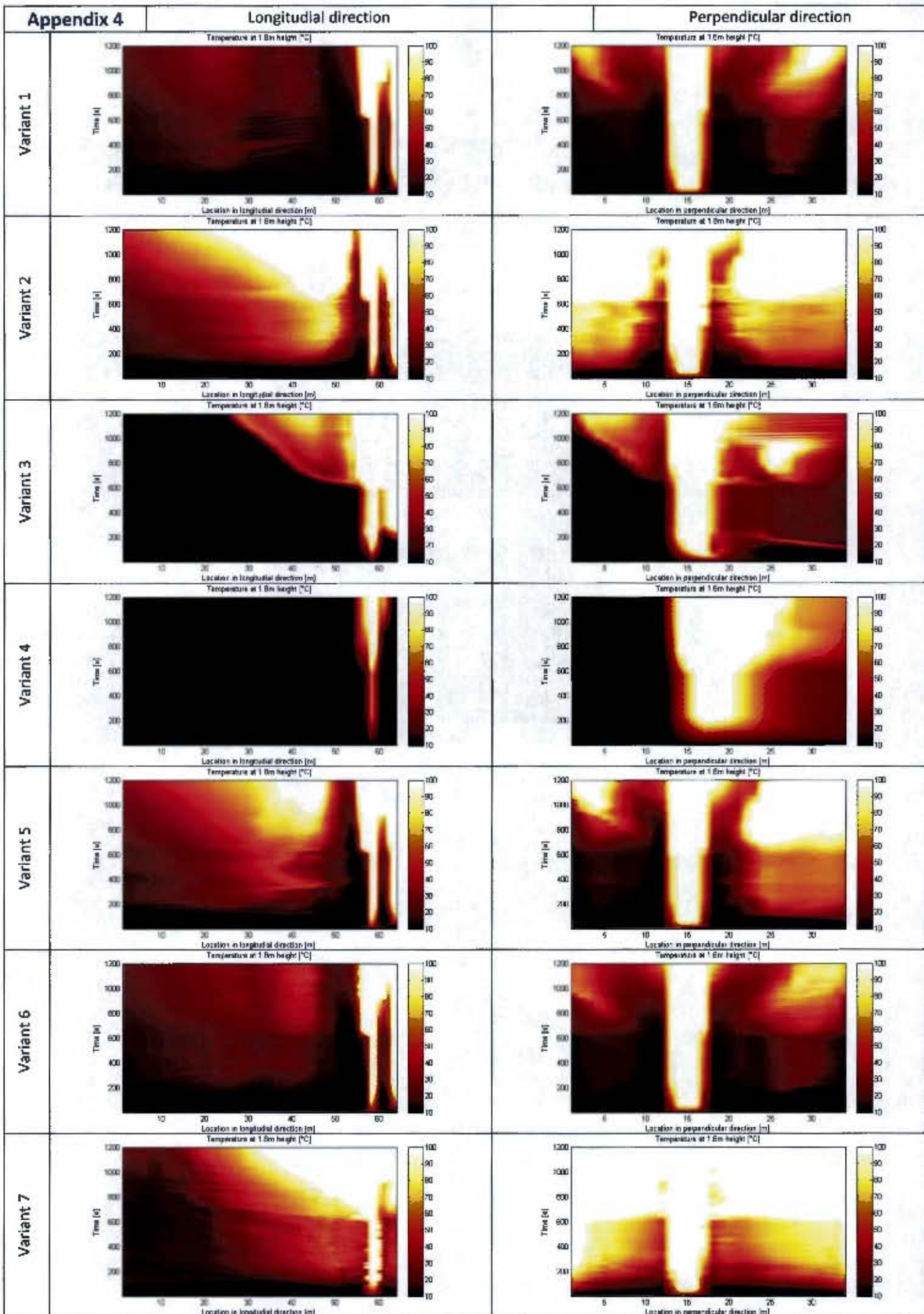


Fig. 64. Determination of border in till where there is visibility towards the fire.



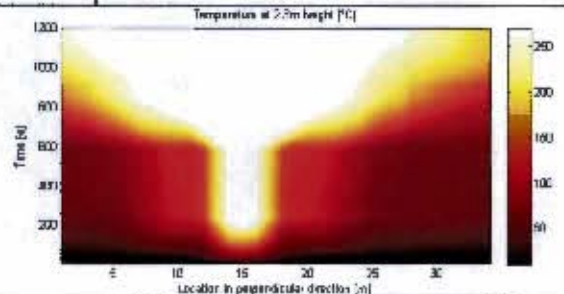
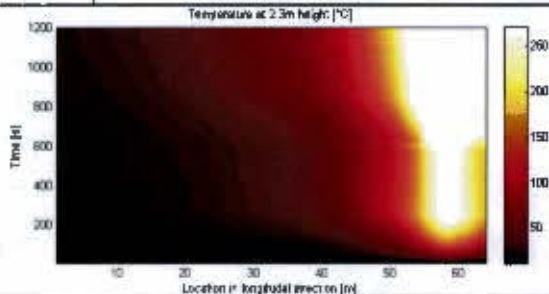


**Appendix 5**

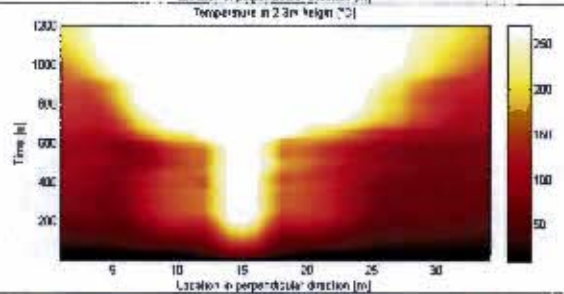
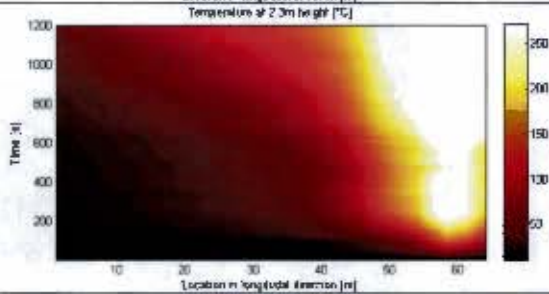
**Longitudinal direction**

**Perpendicular direction**

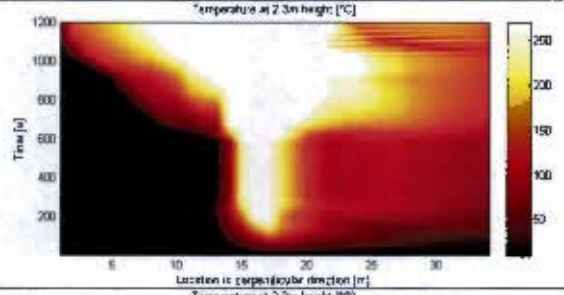
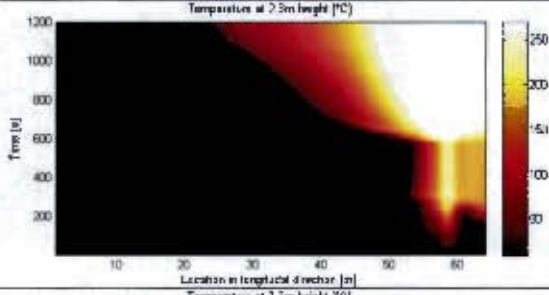
Variant 1



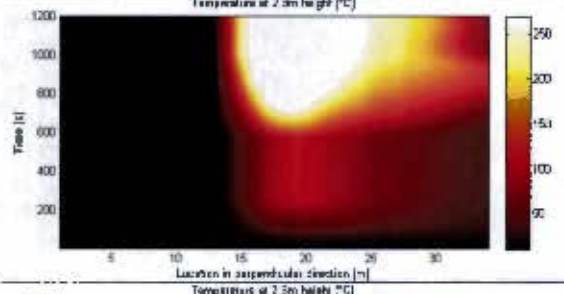
Variant 2



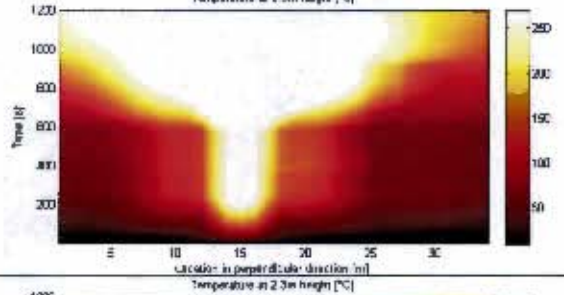
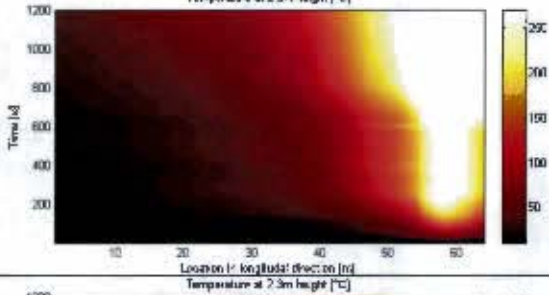
Variant 3



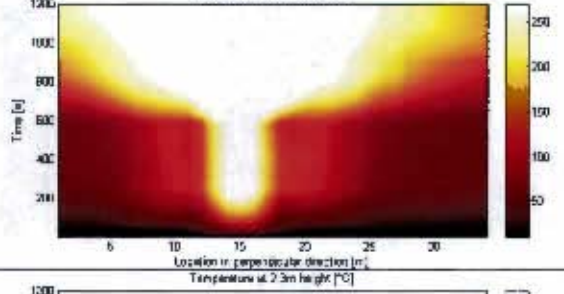
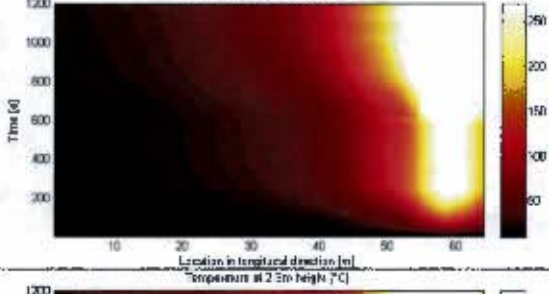
Variant 4



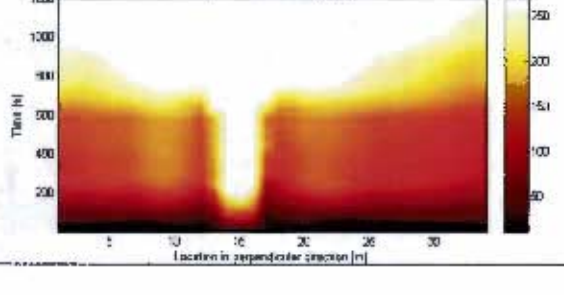
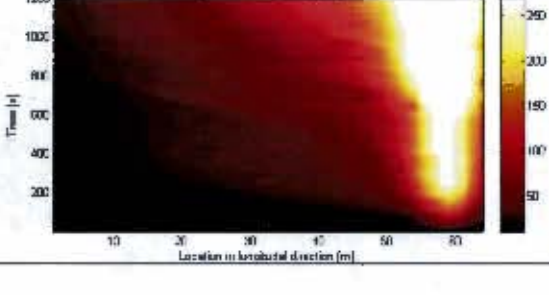
Variant 5

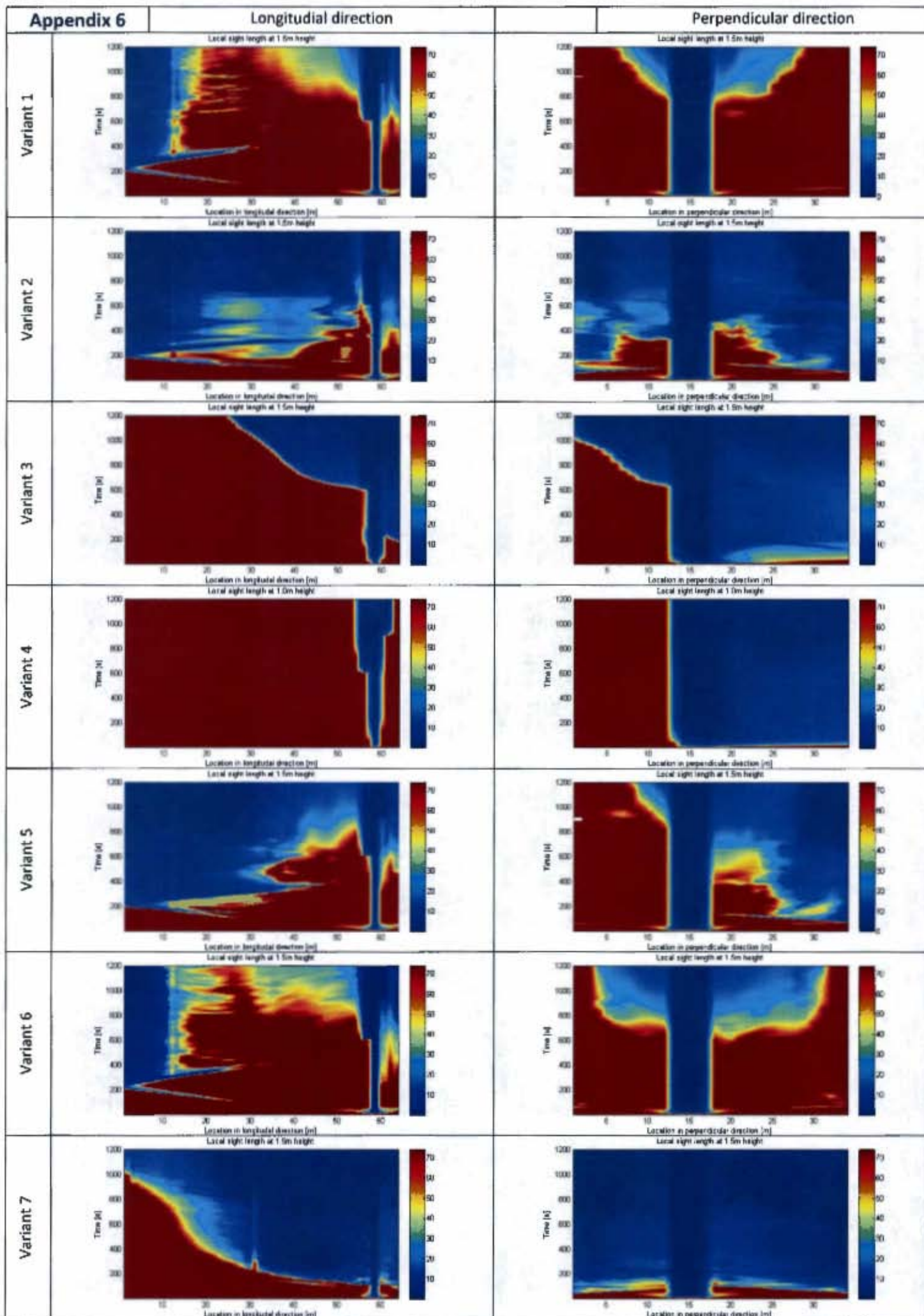


Variant 6



Variant 7



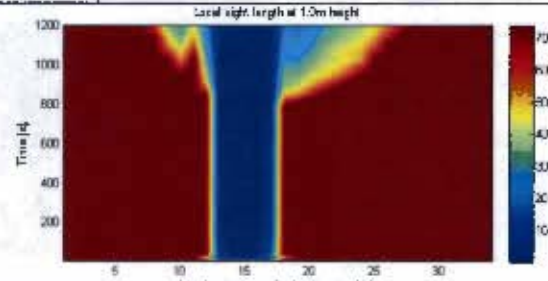
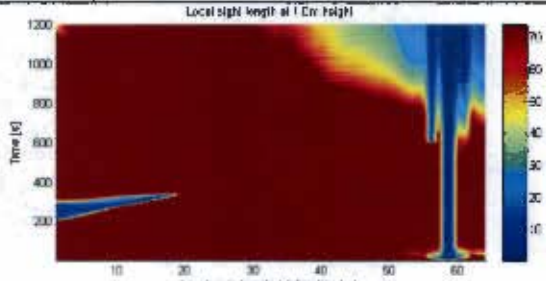


**Appendix 7**

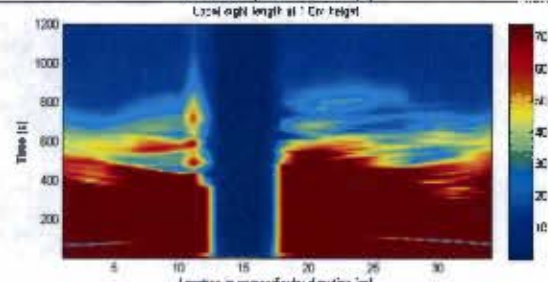
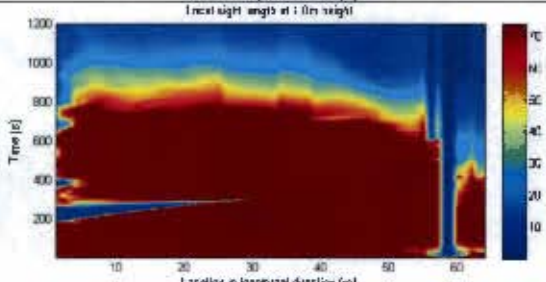
**Longitudinal direction**

**Perpendicular direction**

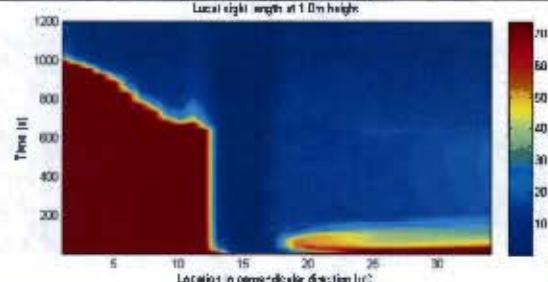
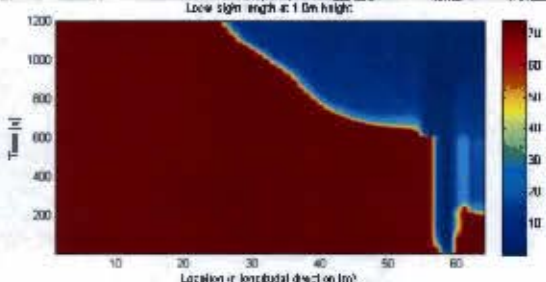
Variant 1



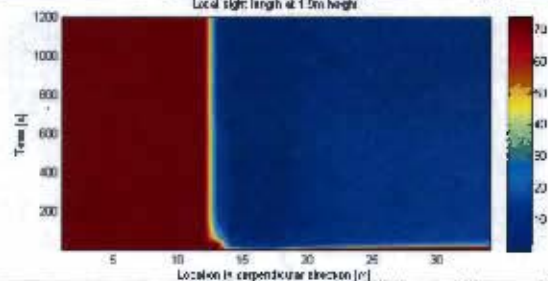
Variant 2



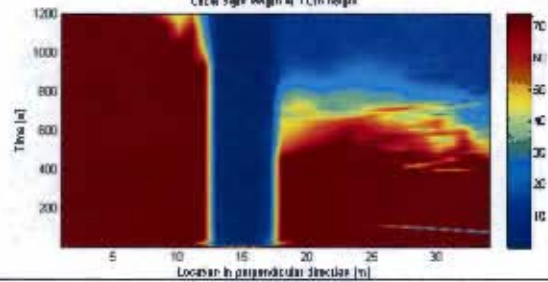
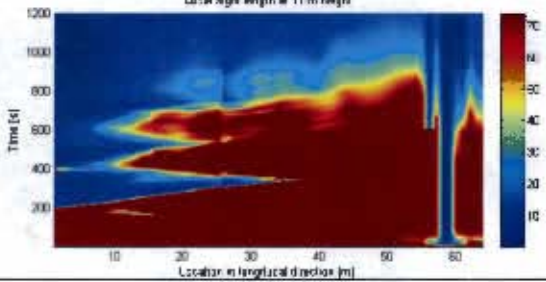
Variant 3



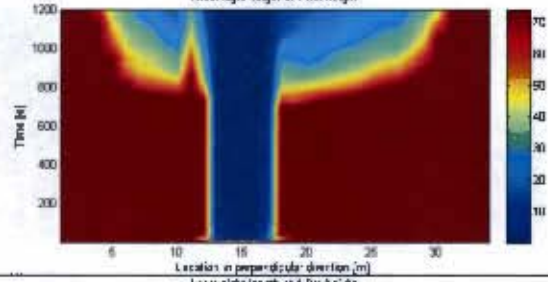
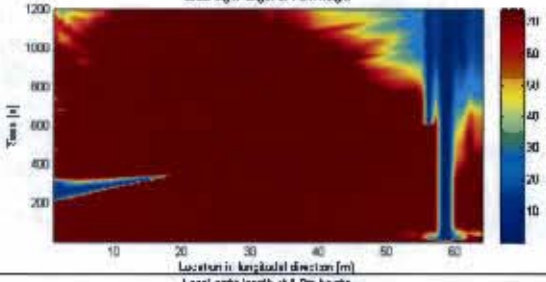
Variant 4



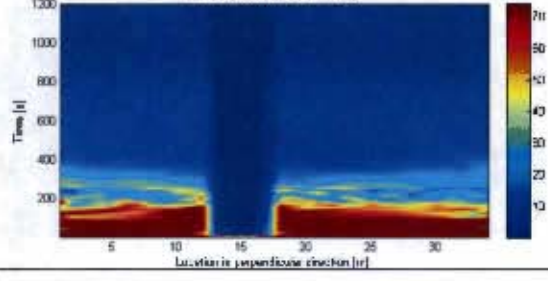
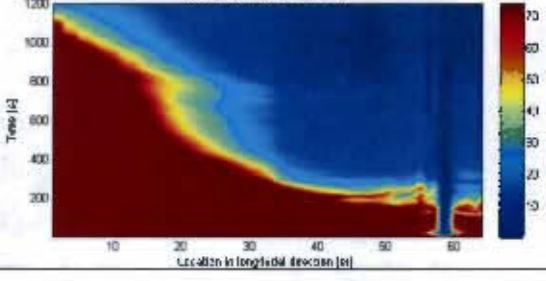
Variant 5

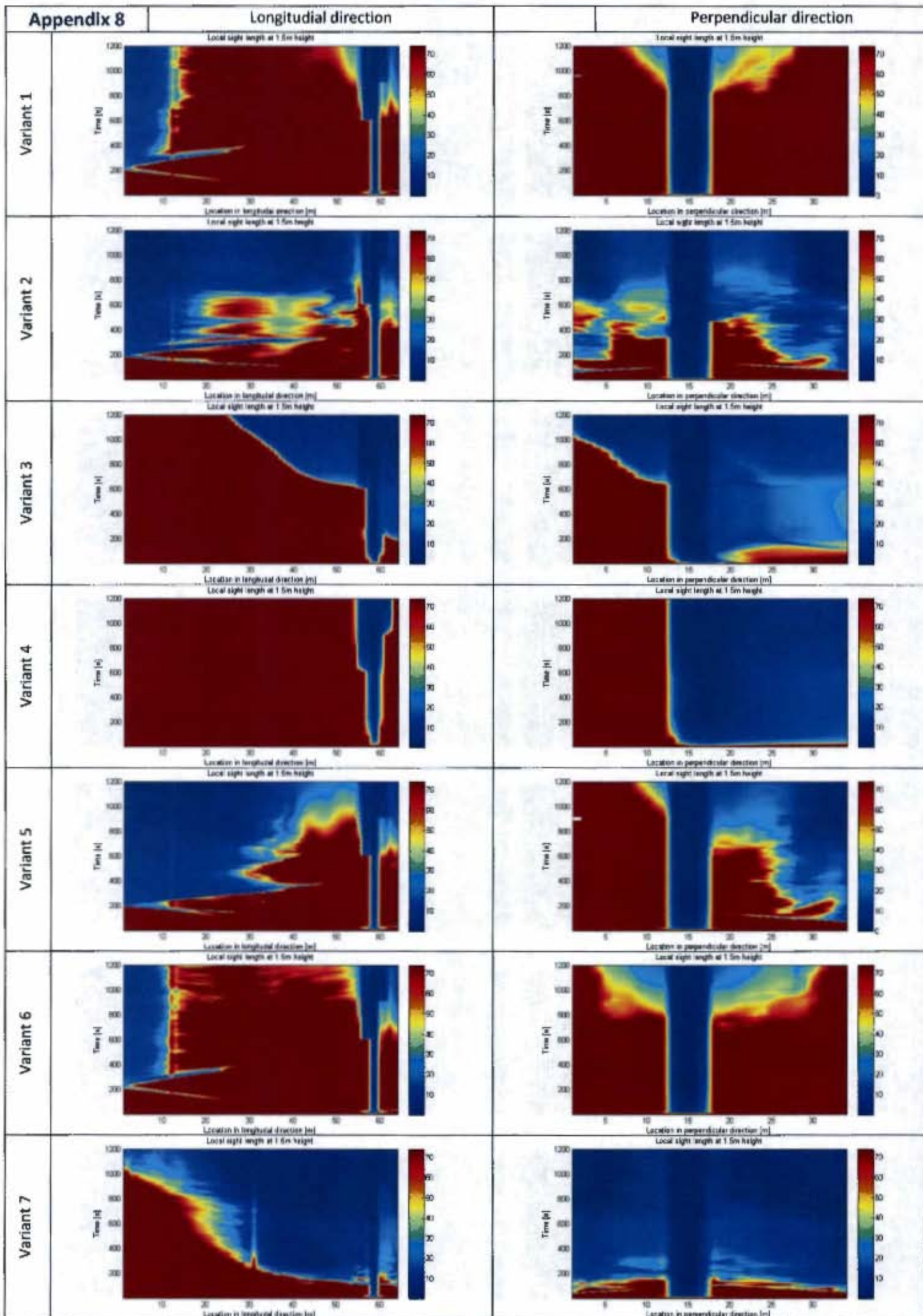


Variant 6



Variant 7



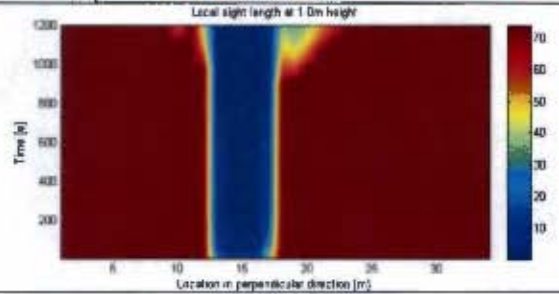
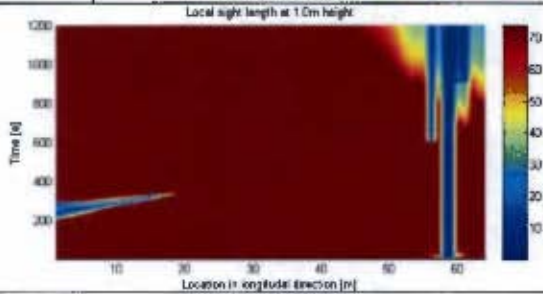


**Appendix 9**

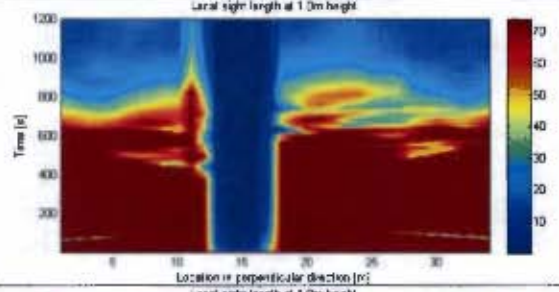
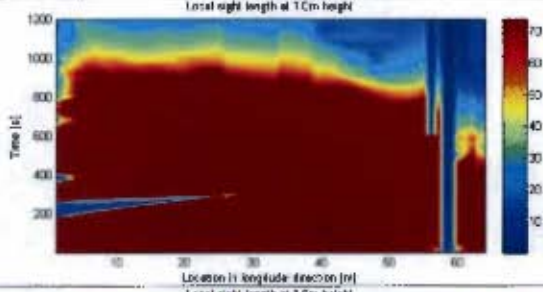
**Longitudinal direction**

**Perpendicular direction**

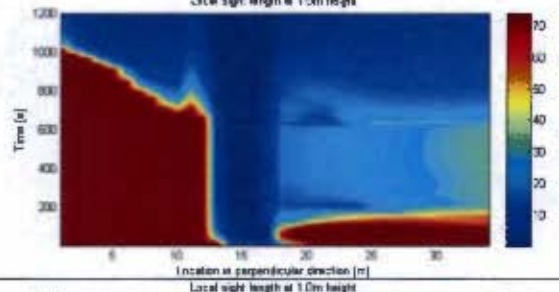
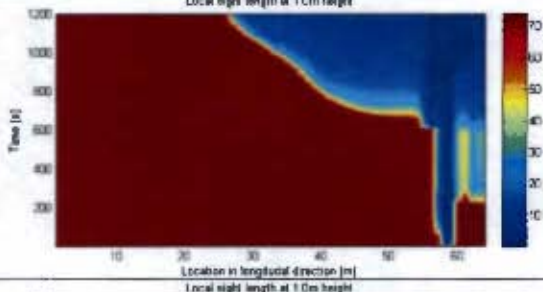
Variant 1



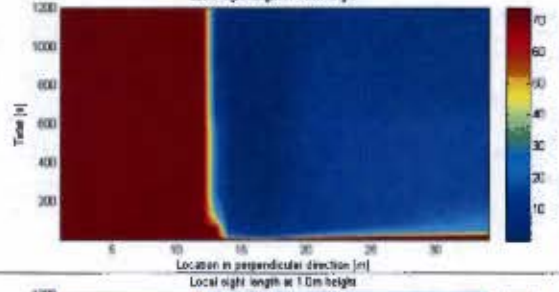
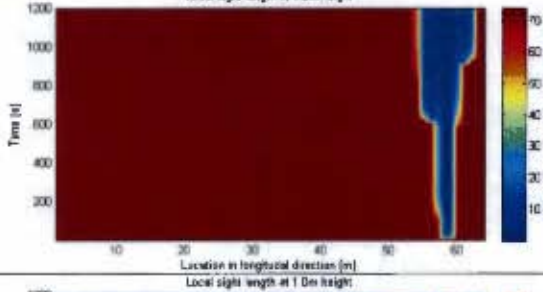
Variant 2



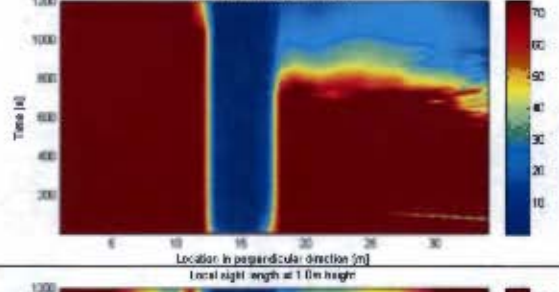
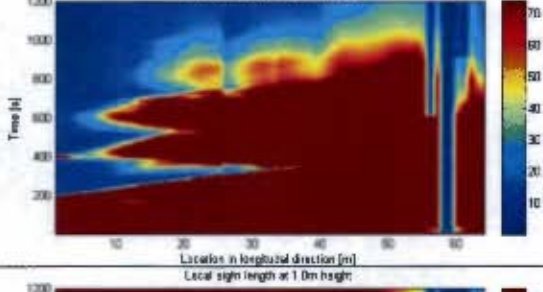
Variant 3



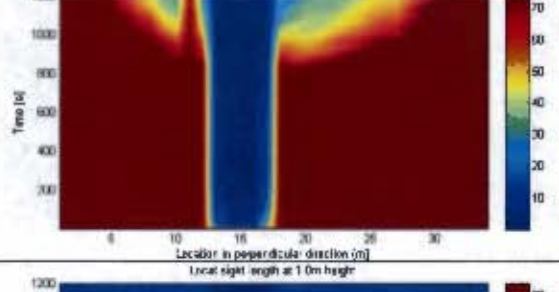
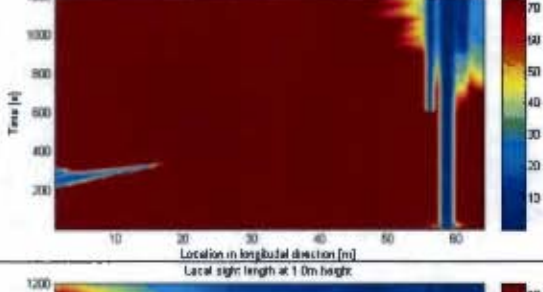
Variant 4



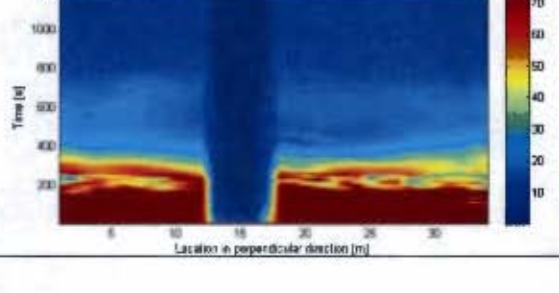
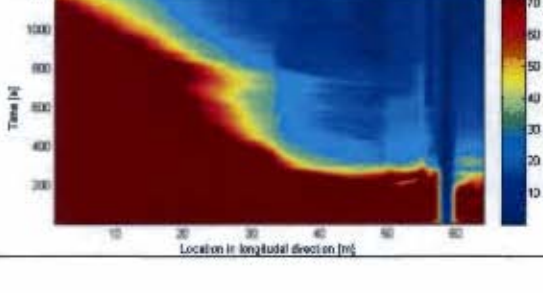
Variant 5



Variant 6



Variant 7



A handwritten signature in black ink, appearing to read 'Mike van der Heijden', written over a horizontal line.

Mike van der Heijden  
*November 2010*